

SAND74-0412
Unlimited Release

High Temperature TKD Thermal Insulation

***When printing a copy of any digitized SAND
Report, you are required to update the
markings to current standards.***

Robert D. Klett

Prepared by Sandia Laboratories, Albuquerque, New Mexico 87115
and Livermore, California 94550 for the United States Energy Research
and Development Administration under Contract AT(29-1)-789

Printed March 1975



Sandia Laboratories

Issued by Sandia Laboratories, operated for the United States Energy Research and Development Administration by Sandia Corporation.

NOTICE

This report was prepared as an account of work sponsored by the United States Government. Neither the United States nor the United States Energy Research and Development Administration, nor any of their employees, nor any of their contractors, subcontractors, or their employees, makes any warranty, express or implied, or assumes any legal liability or responsibility for the accuracy, completeness or usefulness of any information, apparatus, product or process disclosed, or represents that its use would not infringe privately owned rights.

SAND74-0412
Unlimited Release
Printed March 1975

HIGH TEMPERATURE TKD THERMAL INSULATION

Robert D. Klett
Systems Studies Division 4734
Sandia Laboratories
Albuquerque, New Mexico 87115

ABSTRACT

This report describes the analytical development, processing, and testing of tetrakaidecahedral cellular carbon and graphite thermal insulations. Because of the small cell size, thermal radiation does not significantly increase the conductivity of these insulations at high temperatures. Fibers added to the cellular matrix increase the tensile strength.

Summary

High temperature cellular carbon and graphite thermal insulations (TKD) were designed analytically with the aid of a computer program. The insulations were made by carbonizing and graphitizing cork composites of various densities. The closed cells in the insulation are 14-sided with uniform wall thickness and are less than 0.001 inch in diameter. The multitude of small cells block radiation so efficiently that radiant heat transfer through the insulation is negligible even above 5000^oF. The result is that the conductivity of graphite TKD is nearly constant from room temperature to 5000^oF, and the conductivity of carbon TKD increases less with increasing temperature than other refractory insulations that have larger cells. Tensile and compressive strength of TKD is comparable to other carbon foams. The tensile strength of TKD can be increased by adding rayon fibers to the cork composites prior to carbonization. Recommendations are made for the improvement of TKD and applications are suggested.

ACKNOWLEDGMENTS

The author wishes to express his appreciation to H. O. Pierson and J. F. Smatana for their many useful suggestions and for carbonizing the cork composites. The assistance of the following Sandia personnel in processing, testing, and providing input data is also gratefully acknowledged.

R. U. Acton
F. M. Batchelor
R. L. Buckner
R. L. Courtney
R. M. Curlee
S. F. Duliere
E. R. Frye
J. A. Kahn
K. F. Lindell
H. A. Mackay
J. K. Maurin
C. J. Miglionico
L. G. Rainhart
J. D. Theis

CONTENTS

	<u>Page</u>
Summary	3
Acknowledgments	4
Introduction	7
Theory	8
Cork Composites	15
Carbonization and Graphitization	17
Characterization and Test Results	22
X-Ray Diffraction Tests	22
Electron Scanning Micrographs	22
Thermal Conductivity Tests	28
Mechanical Tests	36
Fiber Reinforced TKD	37
Applications	41
Conclusions and Recommendations	42
References	44

ILLUSTRATIONS

<u>Figure</u>	<u>Page</u>
1. Typical high temperature strength increase of graphite.	9
2. Comparative thermal conductivities of typical carbons and graphites.	9
3. Cell sizes required for negligible high temperature radiation heat transfer.	10
4. 14 sided (tetrakaidecahedral) individual cork cell.	11
5. Voids in XXX grade cork.	12
6. Ground and refined cork size 20/40.	15
7. Cork Composites	16
8. Thermogravimetric analysis of composition cork with 22 percent by weight phenolic binder.	18
9. TKD carbonizing cycle based on a thermogravimetric analysis.	19
10. Carbonized TKD	20
11. Machined carbonized TKD	21
12. 13.3 lb/ft ³ carbonized TKD cells.	24
13. Carbonized TKD showing tetrakaidecahedron cells.	25
14. Typical junction of carbonized TKD cell walls.	26
15. TKD graphitized at 3000°C showing a rare wall separation and cigar shaped growths.	27

ILLUSTRATIONS (cont)

<u>Figure</u>		<u>Page</u>
16.	Graphitized 29.5 lb/ft ³ composition cork with phenolic binder showing cell distortion and local cell collapse at a granule boundary.	29
17.	Cut surface of carbonized isolation cork.	30
18.	Fractured surface of graphitized corkboard.	31
19.	Thermal conductivity of carbonized composition cork.	33
20.	Thermal conductivity of graphitized composition cork.	33
21.	Thermal conductivity of carbonized phenolic cork.	34
22.	Thermal conductivity of graphitized phenolic cork.	34
23.	Thermal conductivity comparison of TKD, carbon form, and fibrous carbon.	35
24.	Compressive stress/strain curve for 24.5 lb/ft ³ carbon TKD insulation.	36
25.	Tensile fracture of reinforced carbon TKD showing fiber keying and a granule pull out.	39
26.	Local cell crushing around reinforcing fibers.	40

TABLES

		<u>Page</u>
I	Composition of Cork	13
II	Weight Loss and Shrinkage as a Function of Carbonization Temperature	20
III	Internal Dimensions of TKD and Reference Carbon and Graphite	22
IV	Average Cell Sizes of Carbon TKD	23
V	Thermal Conductivities of Several Carbon and Graphite TKD Insulations	32
VI	Average Electrical Resistivities of Carbon, Graphite, and TKD	36
VII	Comparison of Compressive Strengths of TKD, Carbon Foam, and Fibrous Carbon	37
VIII	Comparative Tensile Strength of TKD and Carbon Foam	38

HIGH TEMPERATURE TKD THERMAL INSULATION

Introduction

Refractory thermal insulations are needed to protect structures, electronics, and personnel in environments such as hypersonic reentry and high temperature processing or experiments. Most of the existing insulations cannot survive these temperatures which can exceed 4000^oF. Insulations that can survive usually have a large increase in conductivity at high temperatures due to radiation heat transfer within the insulation which reduces their effectiveness. In addition to survivability and low conductivity at high temperatures, there are several other desirable characteristics for high temperature insulation. Any structural member that protrudes through the insulation could cause a local hot spot in the protected area; therefore, the insulation should have structural strength. When materials are heated several thousand degrees, thermal expansion becomes a problem. Another desirable property for the insulation is resiliency to compensate for thermal expansion of the insulation and surrounding materials.

The current generation of isotopic heaters used in thermoelectric generators for space application are designed to reenter the earth's atmosphere and contain the radioactive fuel after earth impact (Ref. 1 and 2). The heater structural member must be protected from reentry heating so that it will be strong enough to withstand impact on a hard surface. However, if there is too much insulation around the heater, the heat generated during operation in space will overheat the fuel and structure, causing a failure prior to reentry. Ideally, the insulation should have a high conductivity at the relatively low operating temperatures (about 1000^oF) and a low conductivity at the higher reentry temperatures. This is the opposite temperature/conductivity relationship exhibited by existing low density, low conductivity insulators. There are isotopic heater designs that do function effectively and safely using a combined insulator, support, and compliance member (Refs. 3 and 4), but the designs could be improved if better insulations were available. Insulations used in space nuclear power supplies operate in a vacuum or an inert atmosphere, thus eliminating any oxidation problem; however, the insulation must be compatible with ablation, cladding, and structural materials at elevated temperatures and suffer no degradation from nuclear radiation.

Fibrous and foam carbon insulations are being used for reentry thermal protection. The conductivities of both insulators increase proportionally to T^3 at high temperatures because of internal radiation heat transfer (Ref. 5). Fibrous carbons have very little compressive strength, and the conductivity increases when it is compressed. Carbon foam has a higher conductivity than fibrous carbon for the same density. It is also brittle and cannot be used as a compliance member. Low temperature conductivity of carbon insulators can be increased by graphitization (Ref. 4), but carbon foam made from polyurethane will not graphitize in conventional processes.

These properties of existing insulations lead to the development of the tetrakaidecahedral (TKD) cellular carbon and graphite insulations described in this report.

Theory

Heat is transferred through insulators by solid conduction, gas conduction, radiation, and in some very loose fibers or large cell foams by gas convection. For a given structure, solid material, and temperature, solid conduction heat transfer is proportional to the density of the insulation. For a given structure and temperature, gas conduction is nearly proportional to the void volume. The amount of heat transferred by gas conduction can also be affected by pressure if the cell sizes are very small and/or the temperatures are high. Radiation is proportional to the fourth power of temperature and inversely proportional to the number of radiation shields (i. e., cell walls per unit thickness). Therefore, efficient high temperature insulations must have small void volumes. In addition to these heat transfer considerations, strength, resiliency, high temperature survival, compatibility, ease of manufacture, and cost were also criteria for the insulation being designed.

The strength of a cellular structure is higher than that of fibers, powders, or loose laminates. Flat-sided cells that are loaded in pure tension or compression are stronger than cells which have larger bending moments. Unless cells can be made with heavy structural edges, cells with uniform wall thicknesses are stronger than cells with varying wall thicknesses for a given density.

A sintered or bonded fiber structure is the most resilient, but if a cellular structure is chosen for strength, resiliency must be obtained by proper material selection. Survivability and compatibility are also dependent on material selection. Some of the potential uses for the insulation would be reentry vehicles and reentering isotopic heat sources. Currently, both applications use carbon or graphite ablation shields which can have surface temperatures as high as the sublimation temperatures which range from 5540°R at 10^{-3} atmosphere pressure, 7110°R at 1 atmosphere, to 9450°R at 10^3 atmospheres (Ref. 6). For high temperature survival and compatibility, carbon and graphite would be candidate materials for the insulation. The greatest structural loading on reentry vehicles is during peak deceleration and earth or planet impact when the insulation is hot. Therefore, a material that increases in strength with increasing temperature, such as graphite (Figure 1), is desirable. In the temperature range of interest, the conductivity of graphite decreases with temperature, which would make it well suited for space nuclear power supplies. The conductivity of carbon increases with temperature (Figure 2), but it is lower than graphite conductivity, which would make it a better selection for reentry vehicles with no internal heating. However, most carbons graphitize when they are held at temperatures ranging from 4000 to 6000°R for extended periods of time. Shrinkage occurs during the graphitizing process, which limits the use of these carbon insulators. Graphite has a lower modulus of elasticity and a larger yield strain than carbon and hence is more resilient and compensates better for differential

thermal expansion. Carbon and graphite appeared to be the best materials for the insulation being designed, but other refractories, such as zirconia, magnesia, silica, and alumina, were also investigated.

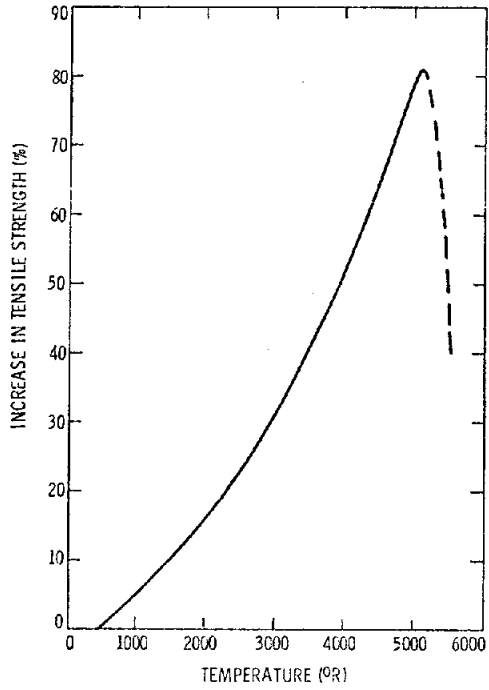
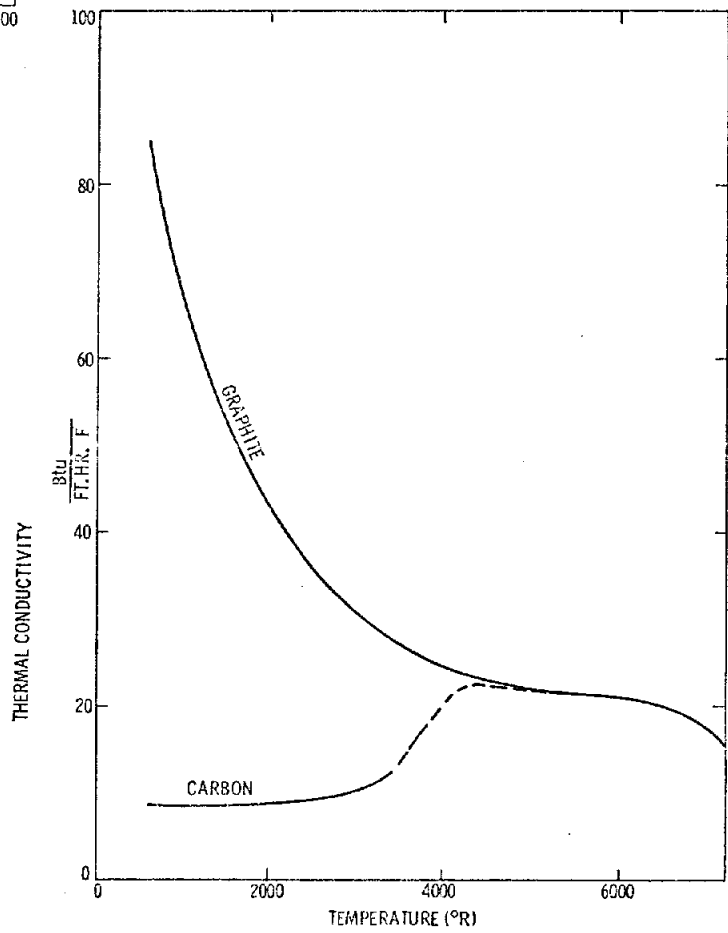


Figure 1. Typical high temperature strength increase of graphite. (Reference 6)

Figure 2. Comparative thermal conductivities of typical carbons and graphites. (References 6, 7, and 8)



The parameters mentioned above were quantified using the INCON computer program described in Reference 9. Parametric runs were made with each material and several cover gases with pressures ranging from a vacuum to 1000 atmospheres. Cell size, cell density, cell alignment, and cell configurations were varied to optimize the insulation. Since radiation is the cause for the increase in conductivity of other insulations at high temperature, radiation blockage was a prime requirement. The curve in Figure 3 shows the maximum allowable cell size of low conductivity, carbon insulations ranging from 5 to 30 lb/ft³ to keep radiation to less than 10 percent of the total heat transferred at 5000°R. Cells 0.001 inch in diameter are acceptable over the practical range of densities. Radiation heat transfer is between 0.62 and 5.9 percent, and gas conduction is between 4.3 and 34.1 percent in carbon and graphite 0.001 inch insulations at 5000°R. The wide range in the conductivities of the different kinds of carbon and graphite account for the range of radiation and gas conduction percentages (Reference 7, Figures 3001 and 3001B). Cells 0.001 inch in diameter will also lower the effective gas conductivity at reduced pressures. As shown by Figure 11 and Eq. (8) of Reference 9, the effective conductivity of air begins to decrease at one atmosphere and becomes negligible at 10⁻³ atmosphere in 0.001 inch cells at 5000°R. At low pressures the conductivity of 0.001 inch carbon or graphite insulation is approximately proportional to the density of the insulation and the conductivity of the solid material.

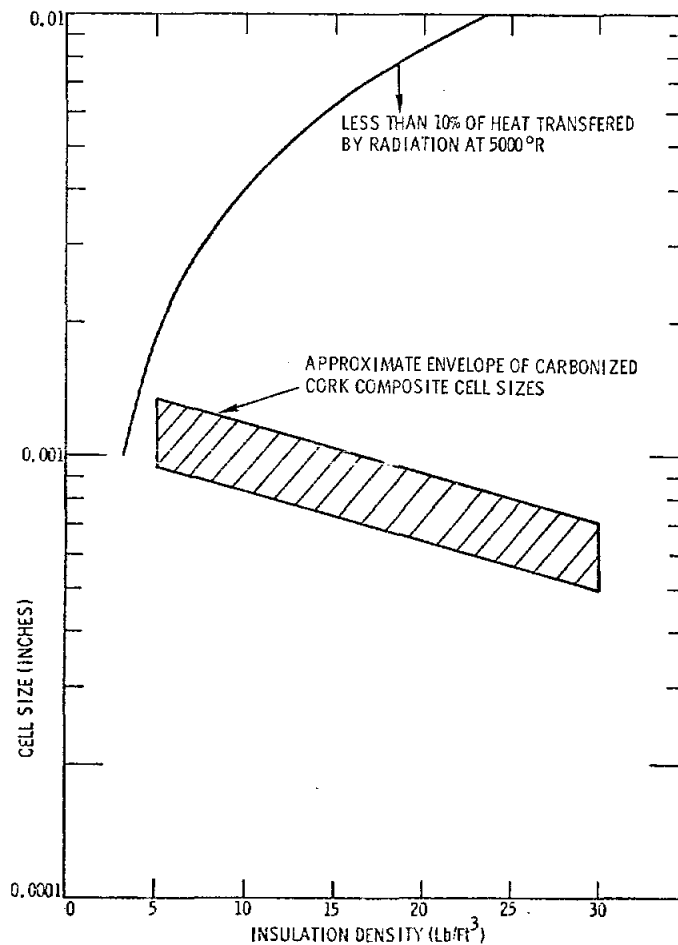


Figure 3. Cell sizes required for negligible high temperature radiation heat transfer. Carbon cellular insulation in 1 atmosphere air.

Other results of the carbon and graphite parametric study include the following.

1. The cells should be staggered to increase the conduction path length in the solid. This would indicate a closely packed structure such as spheres or polyhedrons.
2. The cells should be closed to make full use of the walls as radiation shields. Low density spherical cells may have thin areas that transmit radiation (Ref. 10). No transmission was predicted with uniform thickness walls.
3. Since most of the heat is transferred by solid conduction, the density should be as low as possible while maintaining adequate strength.
4. If the insulation is to be used in an application that requires little or no increase in conductivity with temperature, the material must graphitize or be made of graphite.

Cork has the cell structure selected by the INCON study, but it decomposes between 250 and 900^oF. It has been an efficient low temperature insulation and has recently been used as low heat flux ablation shields (References 11, 12, and 13). When cork is used as an ablation shield, pyrolysis and oxidation take place at a low temperature and a weak, porous, nonhomogeneous char is formed. Although cork could not be used as a high temperature insulation, it could be used as a structural model or possibly as a precursor for the insulation.

Cork is made up of individual 14 sided (tetrakaidecahedral) cells (Figure 4). This configuration gives cork the least possible surface to volume ratio with no interstices. The cells are air filled and are bonded together with lignin which is a resinous binding substance. The size of the cells vary slightly, ranging from 0.0008 to 0.002 inch.

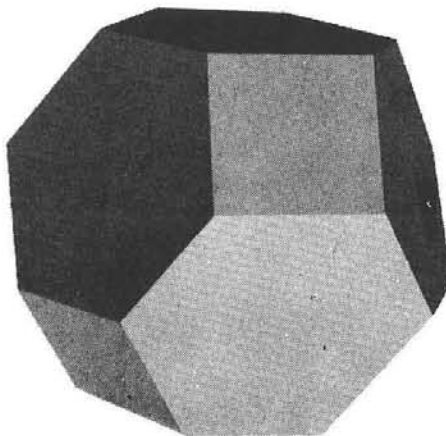


Figure 4. 14 sided (tetrakaidecahedral) individual cork cell.

After cork bark is removed from the tree, it is boiled to remove tannins and other water soluble materials and loose dirt. The hard outer surface is then removed, leaving the cork in its commonly used form. The density is 12.5 to 15.5 lb/ft³ after processing. Even high quality cork has numerous voids (Figure 5). An insulation made from cork in this form would be nonhomogeneous, have low strength, and high conductivity at high temperatures because of radiant heat transfer across the voids. Uniform cork composites can be made by grinding the cork and then bonding the granuels together by any of several processes.

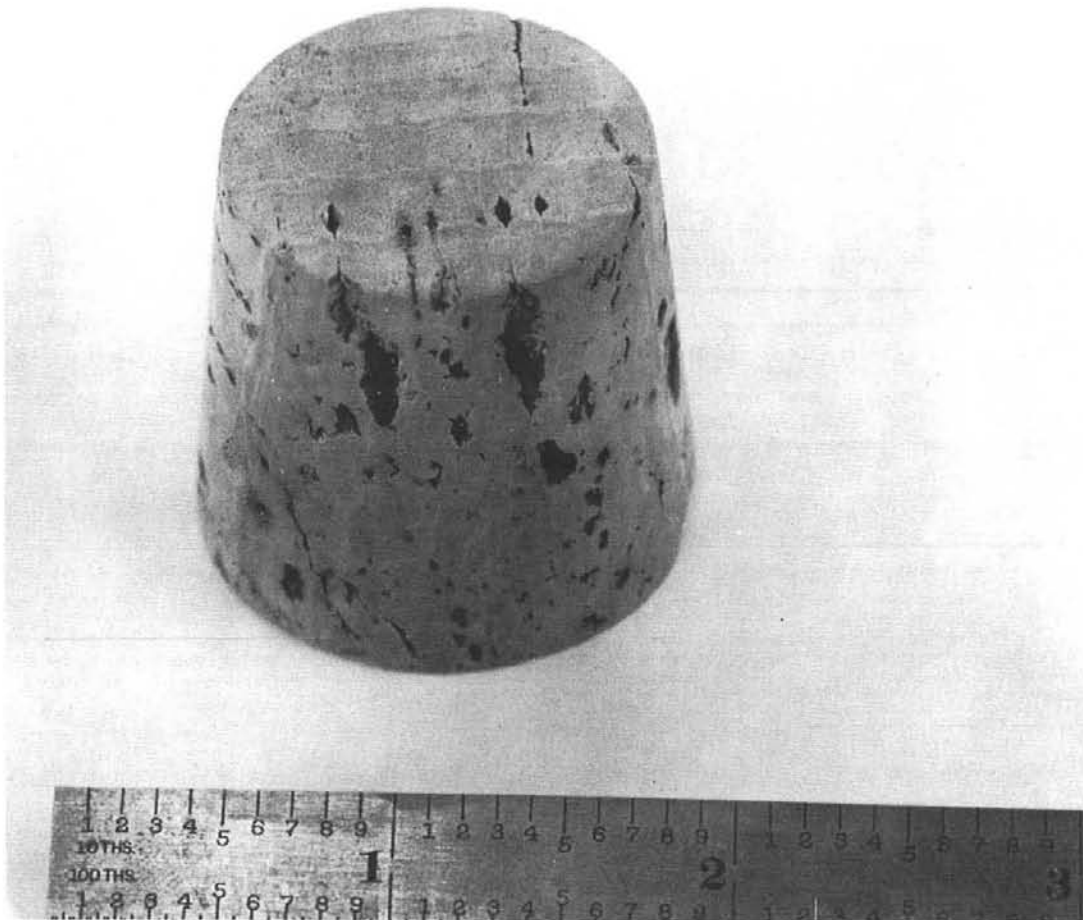


Figure 5. Voids in XXX grade cork. Scale in inches.

The chemical composition of cork is given in Reference 14. Quantitative analysis of cork will vary slightly with the quality and source of the sample. The average composition of good cork is given in Table I. Acids (44 percent) and cellulose like materials (16 percent) are the major constituents of the cells which are bonded together with the lignin (15 percent).

TABLE I
Composition of Cork

<u>Constituent</u>	<u>Average Amount (%)</u>
Moisture	4
Ceroids (Cerin $C_{30}H_{50}O_2$, Friedelin $C_{30}H_{50}O$, Waxes, Glycerides, Stearine, and Free Acids)	10
Tannins	4
Glycerin	4
Fatty Acids	30
(Phellonic Acid, $HOCH(CH_2)_{20}COOH$) 25%	
(Phloionic Acid, $CHOH(CH_2)_7COOH$) 3.5%	
(Phloionolic Acid, $C_{17}H_{32}(CH_2)_3COOH$) 1%	
(Phellogenic Acid, $HOOC(CH_2)_{20}COOH$) 0.5%	
Other Acids	14
Lignin, $C_6H_6O_2(OCH_3)$	16
Cellulose $C_6H_{10}O_5$	3
Cellulose Like Substances	13
Ash (Al, Ba, Ca, Fe, Mg, Mn, K, Na, and Sr)	2

When cellulose is heated in a vacuum, the volatile products of pyrolysis are CO , CO_2 , H_2O , tars, and small amounts of CH_4 and C_2H_4 . At high temperatures free hydrogen is released. The residue is a carbonaceous mass (Ref. 15). Reactions taking place during the pyrolysing of fatty acids include dehydration, decarboxylation, double-bond conjugation, polymerization, dehydro-cyclization, aromatization, dehydrogenation, and degradation by carbon-carbon cleavage (Ref. 16). These reactions produce mostly H_2O , H_2 , and CO_2 volatiles from the fatty acids listed in Table I. This would indicate that a high carbon yield could be expected by the pyrolysis of these fatty acids. Lignin is an amorphous polymer similar to cellulose but with a lower degree of polymerization (Ref. 14). There are several types of lignin, and little is known about the products of pyrolysis except that a carbonaceous char is formed. Most tests to measure the products of pyrolysis of cellulose, fatty acids, and lignin have been conducted in a vacuum where the volatiles were withdrawn from the solid. If pyrolysis takes place in an inert atmosphere, the gas pressure retards the diffusion of the volatile products out of the solid so the products may undergo secondary reactions with the residue. In addition, pressure will retard the escape of the volatiles from the hot zone, so that they will undergo further secondary reactions in the gaseous state. One of the secondary reactions that would increase the carbon yield of the residue would be CO reacting with another oxygen atom to form CO_2 . If pyrolysis takes place in air, oxidation of the volatiles and residue would take place, which would reduce the carbon yield.

Cork is composed mainly of carbon, oxygen, and hydrogen. Since oxygen and hydrogen are the most common volatile products of pyrolysis, there was a good probability that cork could be

carbonized under the right conditions without changing its original structure except for shrinkage. The highest carbon yield was expected if the carbonization takes place in an inert atmosphere such as argon to increase secondary reactions. Pyrolysis is a uniform internal phenomena which requires diffusion of the volatiles to the surface. Since cork cells are closed, a slow carbonizing cycle should be used to allow the volatiles to escape.

The difference between carbon and graphite lies in the spatial arrangement of the carbon atoms. In graphite, the atoms are in a hexagonal close pack structure and all atomic layers are parallel to each other. The interlayer spacing of graphite is 3.35 \AA , and the crystallite size is on the order of 1000 \AA . In carbon, there is a hexagonal arrangement in one plane but the arrangement in the other two planes is random. Interlayer spacing of amorphous carbon is 3.44 \AA , and the crystallite size is about 50 \AA . There is also intermediate semicrystalline or mesomorphic forms between carbon and graphite that have a definite structure in two dimensions but are random in the third (Ref. 6). Graphitization of carbon involves a displacement and rearrangement of layer planes and small groups of planes to achieve three-dimensional ordering. The growth of the planes may be supplemented by the movement of individual atoms or single carbon rings to fill vacancies in existing crystals. The probability of graphitization is related to the existing degree of disorientation and the extent of carbon-carbon binding between layers (cross linking). Graphitization can be enhanced by the presence of oxidizing gases. Preferential oxidation of the more disordered, noncrystalline regions occurs, eliminating cross linking bonds and single layer planes. The ease of graphitizing carbons depends on the mobility of individual layers. Soft carbons graphitize at 4900°F , but hard or glossy carbons may not graphitize until they reach 6300°F because of strong cross links (Ref. 8). The steps in the graphitization of soft carbon are as follows. Calcination takes place between 1800 and 2400°F . The devolatilization and dehydrogenation stabilize the material. Carbon to hydrogen ratios increase from about 20 to greater than 1000. Between 2700 and 3600°F there is a 0.2 to 0.6 percent volumetric expansion. Between 4000 to 4900°F , the graphitization process proceeds more rapidly and is accompanied by a volumetric contraction as crystal growth and interlayer spacing reduction predominate.

Carbons derived from some of the cork constituents are soft, but carbons derived from others, such as cellulose, are hard and retain a turbostratic structure well above 5400°F (Ref. 8). Therefore, it was expected that carbonized cork would only partially graphitize in low temperature graphitizing processes.

Theoretically, cork should carbonize and at least partially graphitize. Both carbonized and graphitized forms of cork should have the thermal, mechanical, and chemical properties that would make them good high temperature insulators.

Cork Composites

As shown in Figure 5, natural cork has too many voids to be used as a precursor for carbonized cork insulation. There are several processes by which cork composites can be made, all of which require the same initial preparation. After the bark is boiled and scraped, it is dried, granulated, and screened to separate the cork according to grain sizes. Ground cork sizes are based on the standard screen sizes the granules will pass through. Figure 6 shows ground cork that will pass through a number 20 screen (0.84 mm) but will not pass through a number 40 screen (0.42 mm). All cork composites need some kind of adhesive to bond the granules together. The object in reconstituting the cork is: (1) to use as little adhesive as possible, (2) to eliminate gaps between granules, (3) and to distort the granules, and hence the individual cork cells, as little as possible. Finely granulated cork distorts the least but uses the most binder because of the large surface to volume ratio. Large granules use less binder, but the large amount of compression needed to eliminate voids completely collapses some of the cells at the granule boundaries. A good comparison is a mixture with sizes from about 50 to 12. The mixture has a good packing density and bonds together well in all of the composite types.

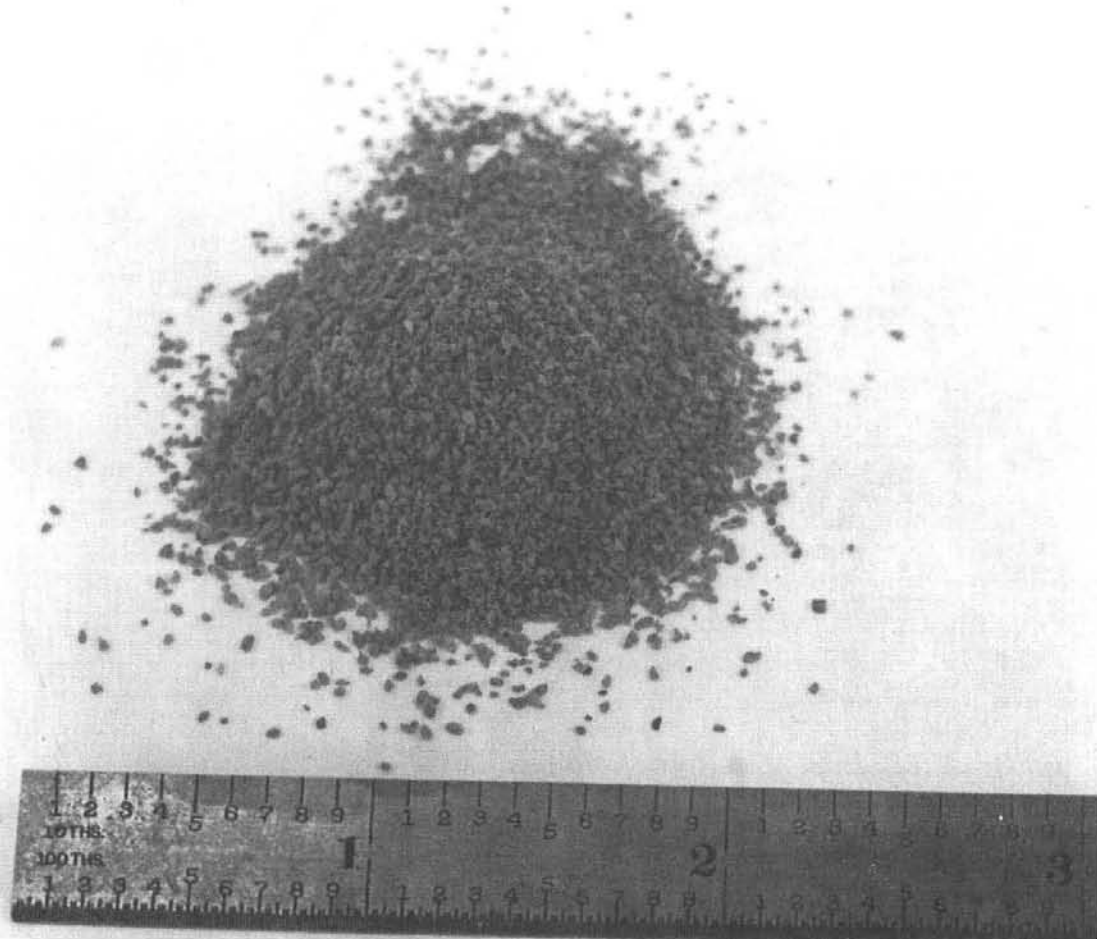


Figure 6. Ground and refined cork size 20/40.

The four basic types of cork composites are composition cork, expanded cork, corkboard, and isolation cork. Composition cork is formed by bonding cork granules together with adhesives. Densities are varied from 7 to 30 lb/ft³ by varying the kind and amount of adhesive, the size of the cork granules, and the amount the mixture is compressed prior to curing. Curing time and temperature depend on the type of adhesive. The adhesive must: (1) have a high carbon yield to retain strength after carbonizing, (2) have a shrinkage during carbonization similar to that of cork to prevent crushing or cracking, (3) wet the cork to obtain a good bond, and (4) have a low viscosity before it is cured so it will flow along granule boundaries and minimize the quantity of adhesive. Thick layers of carbonized adhesive would act as thermal shorts through the insulator. Phenolics, furanes, refined coal tar pitches, and lignin all meet these requirements (Ref. 17). Lignin is the natural cork binder and may be the most compatible with cork granules. Typically, composition cork is about 3 to 6 percent adhesive by volume. Figure 7 shows a block of composition cork made of 16/50 cork with a phenolic binder,

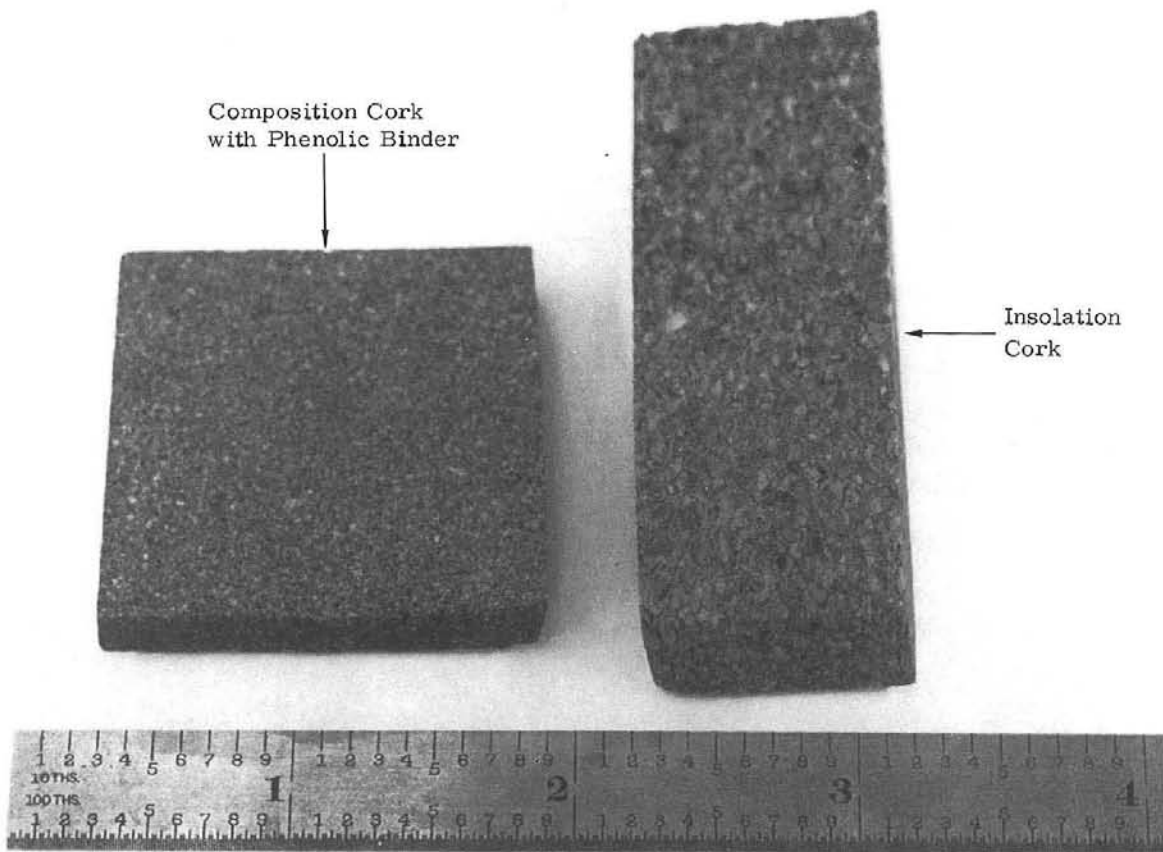


Figure 7. Cork Composites

Corkboard is made without any added adhesive. When cork is heated, it expands and some of the natural resins come to the surface of the granules. Ground and refined cork is placed in a

mold and heat is applied. The pressures created by the expanding cork, force the cork to spread into the voids between particles. The natural resins then resolidify forming a united mass. The expansion of the cork cells gives a product of low density and helps to key the particles together. The heat applied is sufficient to darken the cork cell walls and to remove some of the more volatile constituents, but the air-filled cells remain intact. Densities vary from 5.5 to 14 lb/ft³ depending on the amount of cork loaded into the mold. The cork is heated to between 500 and 600°F and held for 4 to 6 hours at that temperature depending on the thickness of the mold.

Isolation cork is used for machinery mounts. Most commercial isolation cork is low quality with inclusions of the hard outer shell and other impurities. Granule sizes are about number 30 to 6 (Figure 7). Isolation cork is made the same as corkboard except the cork is compressed mechanically in the molds prior to heating to obtain higher final densities which range from 13 to 21 lb/ft³. The compression causes the cells to flatten slightly.

Expanded cork, which has a density of 4 to 6 lb/ft³, is formed by adding calcium carbide to fine cork granules. Acetylene gas is formed and the pressure expands the cells. The granules are then bonded together with adhesives or by heating in a mold. TKD insulation has not been made from expanded cork, but it should be a good precursor for low density TKD.

Cork composites used as precursors for TKD insulation should be formed to approximately desired shape to reduce the amount of material to be carbonized and to minimize the distance that volatiles must diffuse during carbonization. Allowances must be made for the shrinkage and distortion that takes place during carbonization and graphitization. Cork composites machine easily and cleanly. Small parts can be machined from blocks of the composite. Large parts can be molded to the desired shape. Some thin pieces with large radii of curvature can be made by bending sheets of the composites over forms. After carbonization, the rigid insulation will retain its shape.

Refined granulated cork and cork composites are inexpensive and can be obtained from many commercial sources (Ref. 18).

Carbonization and Graphitization

The first attempts at carbonizing cork were with standard cycles in one atmosphere of argon. The cycles were 48 and 78 hours long and had a maximum temperature of 800°C. Chemical analyses indicated that cork does not completely carbonize in a 800°C cycle, so a cycle was developed based on a thermogravimetric analysis (TGA). TGA's were conducted in a vacuum and in an inert atmosphere. The results are shown in Figure 8. At temperatures below 500°C, the results of the tests are almost identical to those given in Reference 19. However, above 500°C, Reference 19 shows almost no weight loss but the weight loss is substantial in Figure 8. Final weight loss in a vacuum is 99 percent in the Sandia test and 82 percent in the Armstrong test.

Sandia measured an 85 percent weight loss in helium, and Armstrong had a 72 percent loss in nitrogen. In both sets of tests, the carbon yield was higher in an inert atmosphere than in a vacuum. It was found that a post cure of the composition cork at 200°C for four hours in air increased the carbon yield slightly. Theory also suggests the yield might be increased with catalysts or by increasing the pressure of the inert cover gas, but these modifications have not as yet been tried.

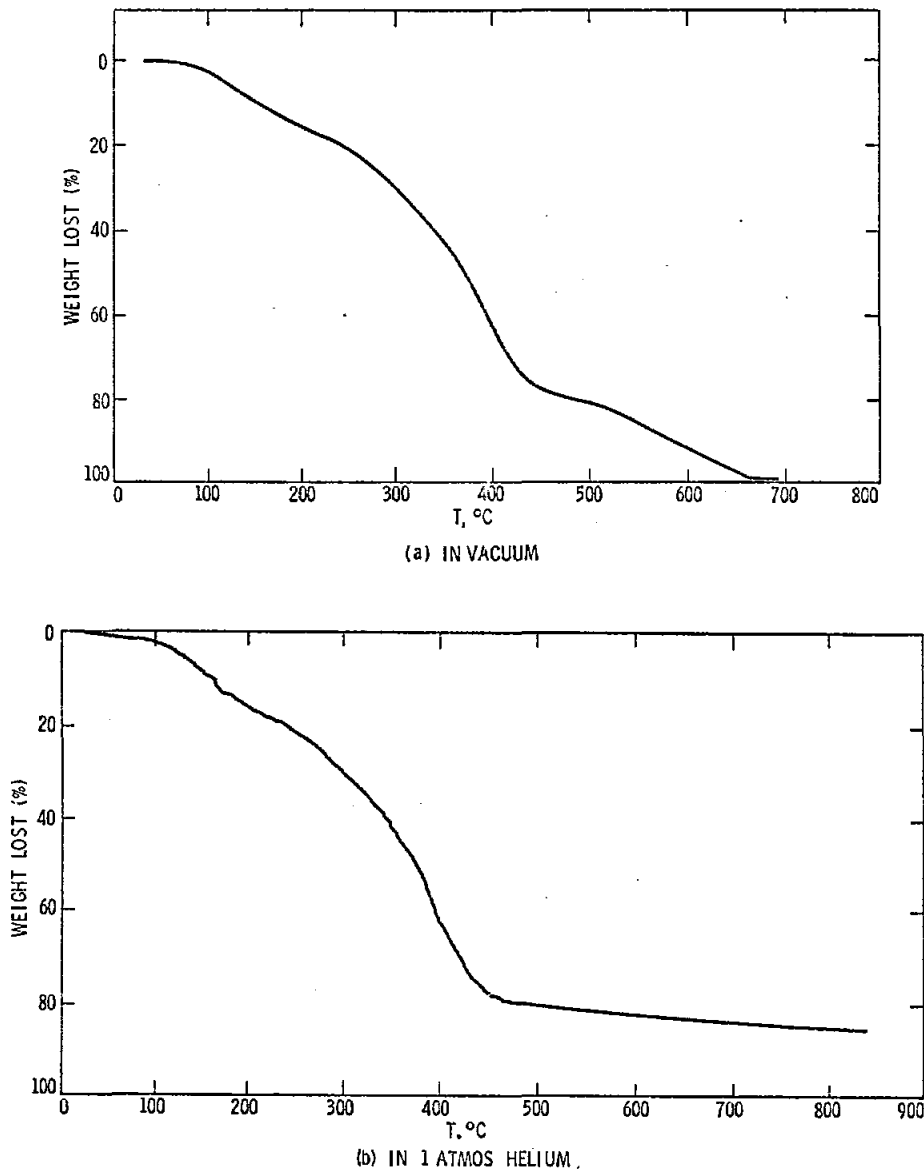


Figure 8. Thermogravimetric analysis of composition cork with 22 percent by weight phenolic binder. Heating rate = 6°C/min.

The carbonizing cycle shown in Figure 9 was based on Figure 8b. The cycle time in a given temperature range is proportional to the mass loss in that range, which produces uniform gas diffusion rates throughout the cycle. The temperature gradient in the composite being carbonized must be small to prevent cracks caused by earlier shrinking of hotter exposed surfaces. Therefore, thicker sections require longer cycles. Longer cycle times are also required for thick sections because of the longer diffusion lengths. Cycle times range from 24 hours for thin samples to 100 hours for 4-inch thick sections. The maximum temperature is held for 1.5 to 6 hours to assure uniform carbonization.

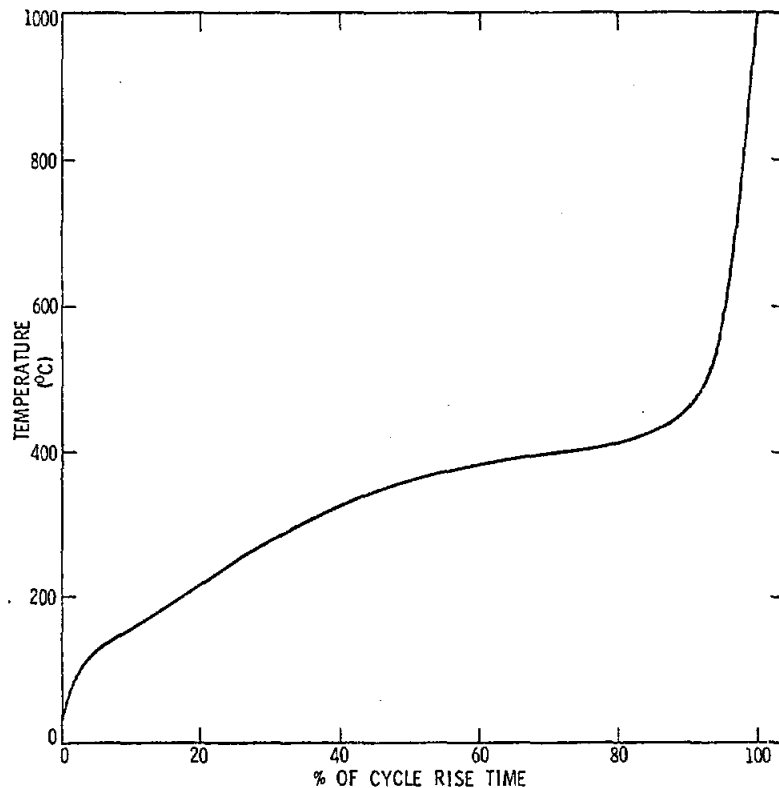


Figure 9. TKD carbonizing cycle based on a thermogravimetric analysis.

Maximum carbonizing cycle temperatures were varied from 800°C to 1400°C. The cover gas was one atmosphere of argon, and the samples were 30 lb/ft³ composition cork with a phenolic binder. Weight losses and shrinkage are given in Table II.

Weight loss is negligible above 1000 to 1100°C, and carbonization is almost complete. The density of carbonized TKD is slightly over 18 lb/ft³ for all carbonizing temperatures.

TABLE II

Weight Loss and Shrinkage as a Function
of Carbonization Temperature

<u>Maximum Temp. (°C)</u>	<u>Fraction of Initial Weight</u>	<u>Fraction of Initial Length</u>	<u>Fraction of Initial Volume</u>
800	0.249	0.74	0.41
900	0.245	0.74	0.41
1000	0.242	0.73	0.39
1100	0.240	0.73	0.39
1200	0.239	0.73	0.39
1300	0.239	0.73	0.39
1400	0.238	0.73	0.39

Cork boards ranging in density from 7.15 to 14.50 lb/ft³ were also carbonized at 1000°C. The fractions of initial weight were 0.29 to 0.30, the fraction of initial length were 0.74 to 0.71, fractions of initial volume were 0.40 to 0.36, and carbonized densities were 5.18 to 12.1 lb/ft³. The cork board had slightly less weight loss and slightly more shrinkage than the composition cork. Shrinkage of carbonized isolation cork was almost the same as cork board, but weight losses were slightly higher, probably due to impurities in the samples. Figure 10 shows carbonized composition cork and isolation cork samples similar to the cork composites in Figure 7.

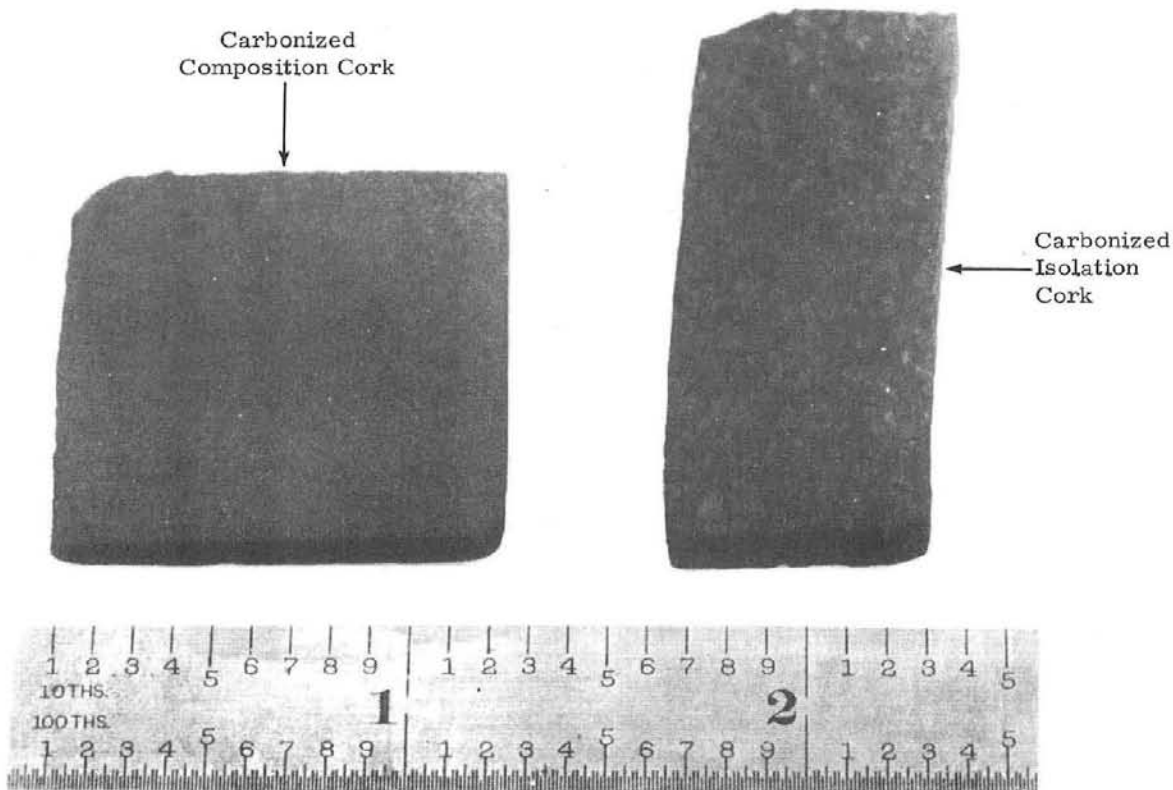


Figure 10. Carbonized TKD

The first samples of TKD were graphitized at 2750°C in one atmosphere of argon. X-ray diffraction tests showed that the samples were only partially graphitized. Subsequent graphitizing cycles with a maximum temperature of 3000°C produced TKD that was more fully graphitized, but graphitization was still not complete. Even higher graphitizing temperatures would be needed to assure no shrinkage if the insulation is used above 3000°C. The graphitization cycles consisted of a rapid rise in temperature up to the maximum temperature of the carbonizing cycle followed by a slow linear increase in temperature through graphitization and a 2-hour hold at maximum temperature.

Composition cork with a phenolic binder that was carbonized at 800°C had an additional weight reduction of 11 percent and a length reduction of 9 percent when it was graphitized at 2750°C. Isolation cork carbonized at 1000°C had a weight reduction of 5 to 7 percent and a length reduction of 10 to 12 percent when it was graphitized at 3000°C.

Since TKD shrinks slightly during graphitization, insulation which is used above 1000°C would have to be graphitized or heat treated at the operational temperature if shrinkage could be detrimental.

All carbonized and graphitized TKD insulations machine easily and have good surface finishes. Figure 11 shows two parts that were rough machined from a block of isolation cork, carbonized, and then machined to final dimensions.

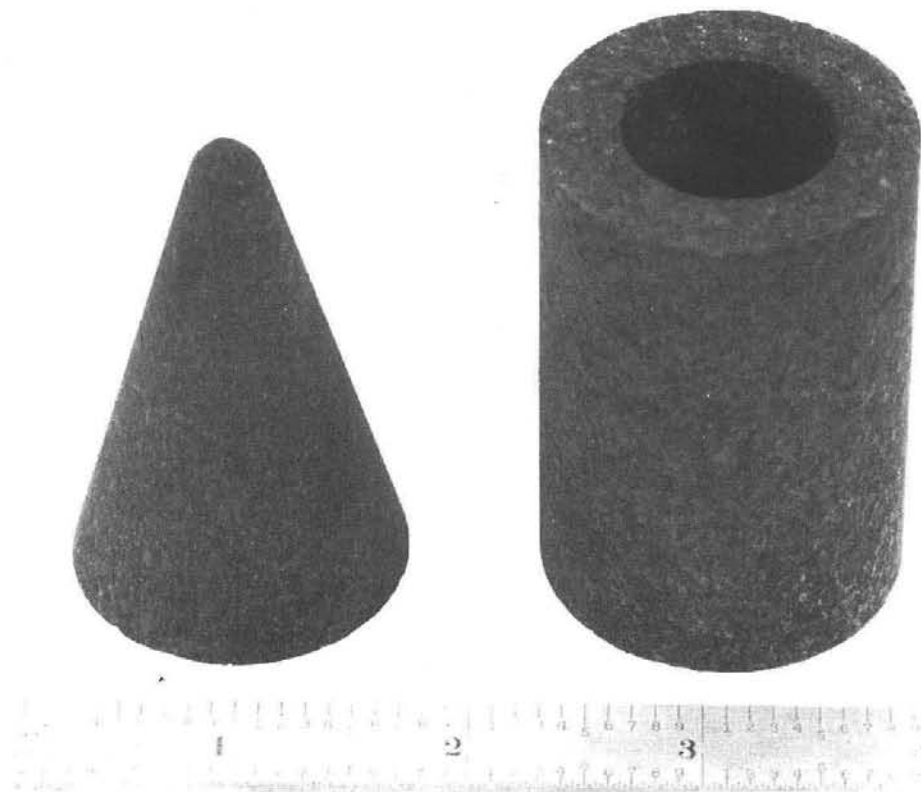


Figure 11. Machined carbonized TKD

Characterization and Test Results

The TKD insulation design was evaluated using: (1) X-ray diffraction tests to determine the degree of graphitization, (2) electron micrographs to observe cell sizes and shapes, wall thicknesses and continuity, and granule interface conditions, (3) thermal conductivity tests to measure the effectiveness, and (4) tensile and compression tests to measure strength, elasticity, and failure modes.

X-Ray Diffraction Tests

The low temperature thermal conductivities of TKD carbonized at 800°C and graphitized at 2750°C were lower than predicted values (Ref. 9), indicating that the carbonizing and graphitizing processes were not complete. X-ray diffraction tests were then conducted on the samples to measure interlayer spacing and crystallite size. The results are shown in Table III along with these parameters for pure carbon and graphite.

TABLE III
Internal Dimensions of TKD
and Reference Carbon and Graphite

<u>Material</u>	<u>d002 Interlayer Spacing (Å)</u>	<u>Crystallite Sizes (Å)</u>
Carbon	3.44	50
Graphite	3.35	1000
TKD (800°C)	3.94	--
TKD (2750°C)	3.43	50
TKD (3000°C)	3.39	90

These tests showed that the 800°C cycle did not form a pure carbon structure and graphitization had only begun at 2750°C. Graphitization was not complete at 3000°C, but the degree of graphitization was sufficient to produce the desired low temperature thermal conductivity. A higher cycle temperature would be needed for more complete graphitization.

Electron Scanning Micrographs

Cell sizes, shapes, and wall thicknesses were needed in order to check the thermal model against experimental conductivity data. All of this information was obtained from electron scanning micrographs of cork composites, carbon TKD, and graphite TKD of various densities. The effects on the shape of the cells and the distortion along granule boundaries caused by compressing or expanding the cork were also determined with micrographs. Other uses of micrographs include measurements of adhesive thicknesses and distribution, location of fractures caused by processing, and determining failure modes of mechanical tests.

Figure 12 shows the structure of a typical section of low density carbon TKD made from cork board. The granules were only slightly compressed during the processing, and the cell distortion is minimal. Cork cells have 6 square and 8 hexagonal flat surfaces. Figure 13 shows this cell shape. The small particles are dust from the sanded surface. Individual walls are uniform in thickness, and the lignin that bonds individual cells together carbonizes to form a single wall between cavities as shown in Figure 14. A rare partial cell wall separation is shown in Figure 15 which illustrates that cork is made of individual cells that are bonded together. Also shown in Figure 15 are cigar shaped growths that formed in some of the cells during a 3000°C graphitizing cycle. Most of the growths are small, and hence little material is removed from the cell walls in their formation. Similar growths on carbon and graphite have been noted previously (Ref. 20).

The average wall thickness of cork was found to be about 0.0001 inch, which agrees with values published in the literature. Average wall thicknesses of carbonized and graphitized cork were about 0.00005 inch. Figure 14 shows an extreme variation in wall thickness. Wall thicknesses of carbon and graphite TKD can also be computed using

$$\text{Carbon Thickness} = \text{Cork Thickness} \left(\frac{\rho_{\text{Carbon}}}{\rho_{\text{Cork}}} \times \frac{\text{Length Carbon}}{\text{Length Cork}} \right)$$

or using the weight reduction and shrinkage from Table II,

$$\text{Carbon Thickness} = \text{Cork Thickness} \left(\frac{\text{Weight Fraction}}{(\text{Length Fraction})^2} \right)$$

For a 1000°C carbonization temperature,

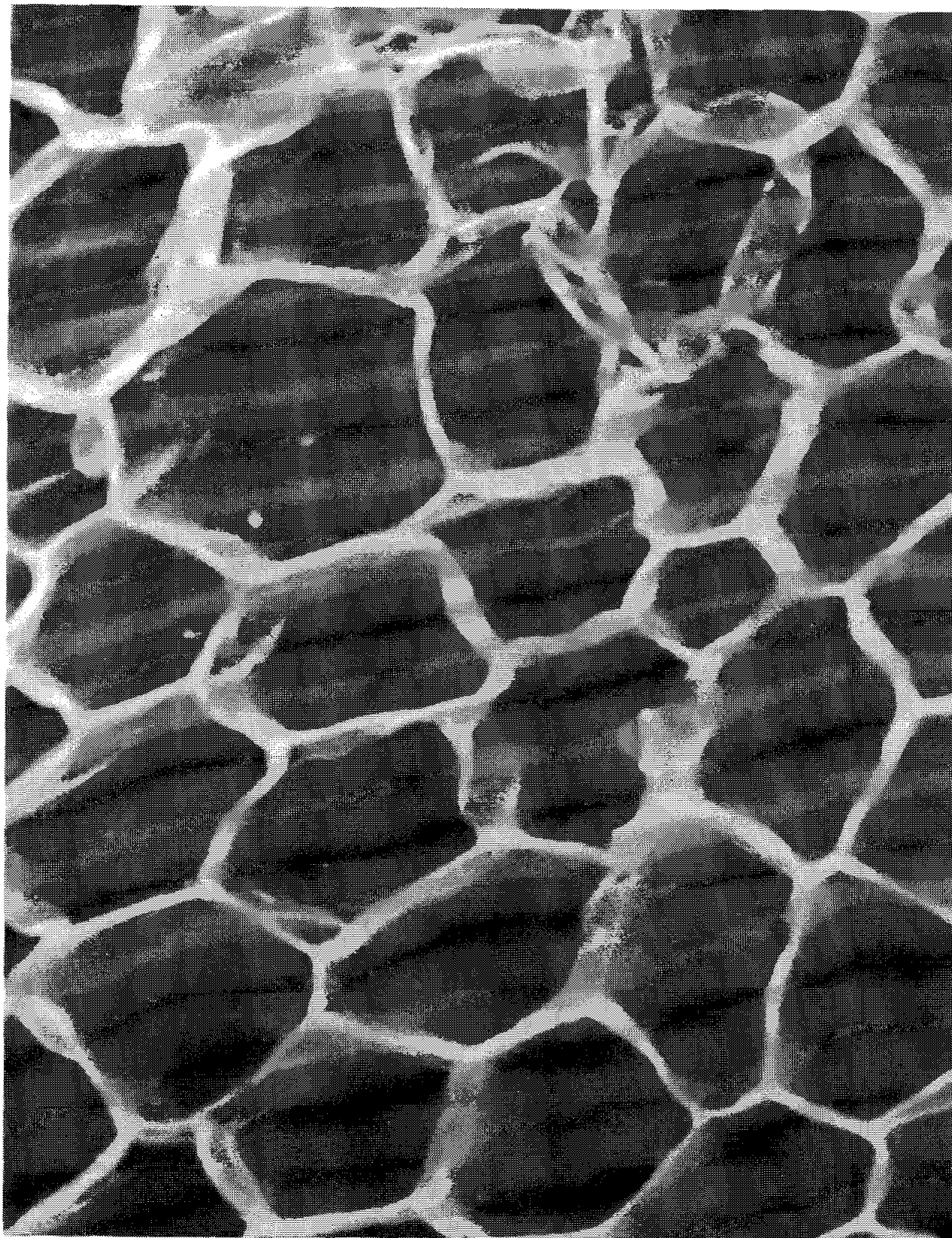
$$\text{Carbon Thickness} = 0.0001 \left(\frac{0.242}{(0.73)^2} \right) = 0.000045 \text{ inches.}$$

The wall thickness is reduced during carbonization by a larger amount than the wall lengths (0.45 of original thickness and 0.73 of original length).

Cells in high density cork composites are crushed more than the cell in low density composites. Defining the cell size as the average of the crushed direction and the two uncrushed directions, average cell sizes of several carbon TKD's are given in Table IV. Also given are the average ratios of cell dimensions in crushed and uncrushed directions (Y).

TABLE IV

Average Cell Sizes of Carbon TKD			
Precursor	Precursor Density (lb/ft ³)	Cell Size (in)	Y
Cork Board	14.5	0.00090	0.90
Isolation Cork	21	0.00075	0.80
Composition Cork	30	0.00070	0.75



0.001 in.

Figure 12. 13.3 lb/ft³ carbonized TKD cells.

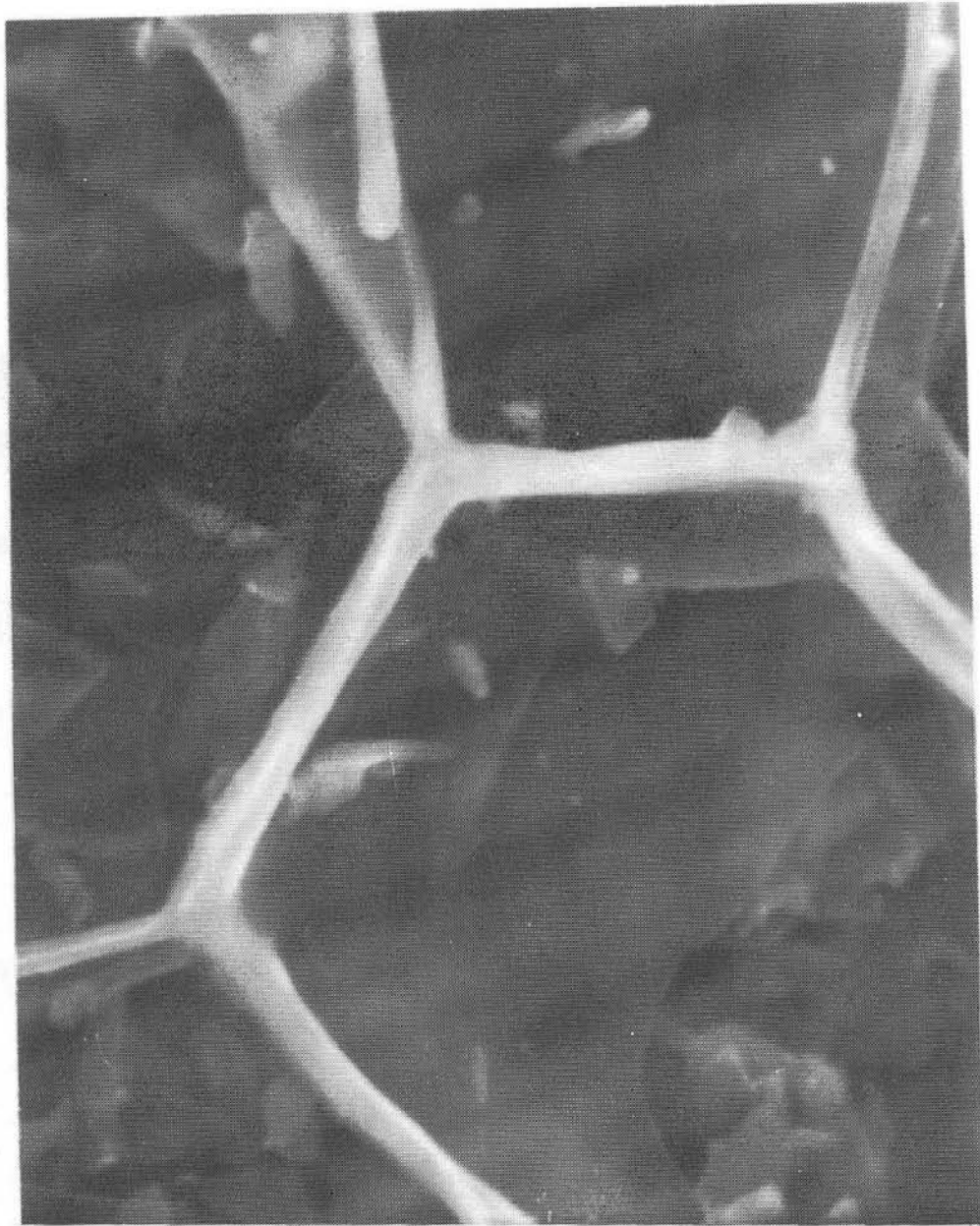


Figure 13. Carbonized TKD showing tetrakaidecahedron cells.



Figure 14. Typical junction of carbonized TKD cell walls.

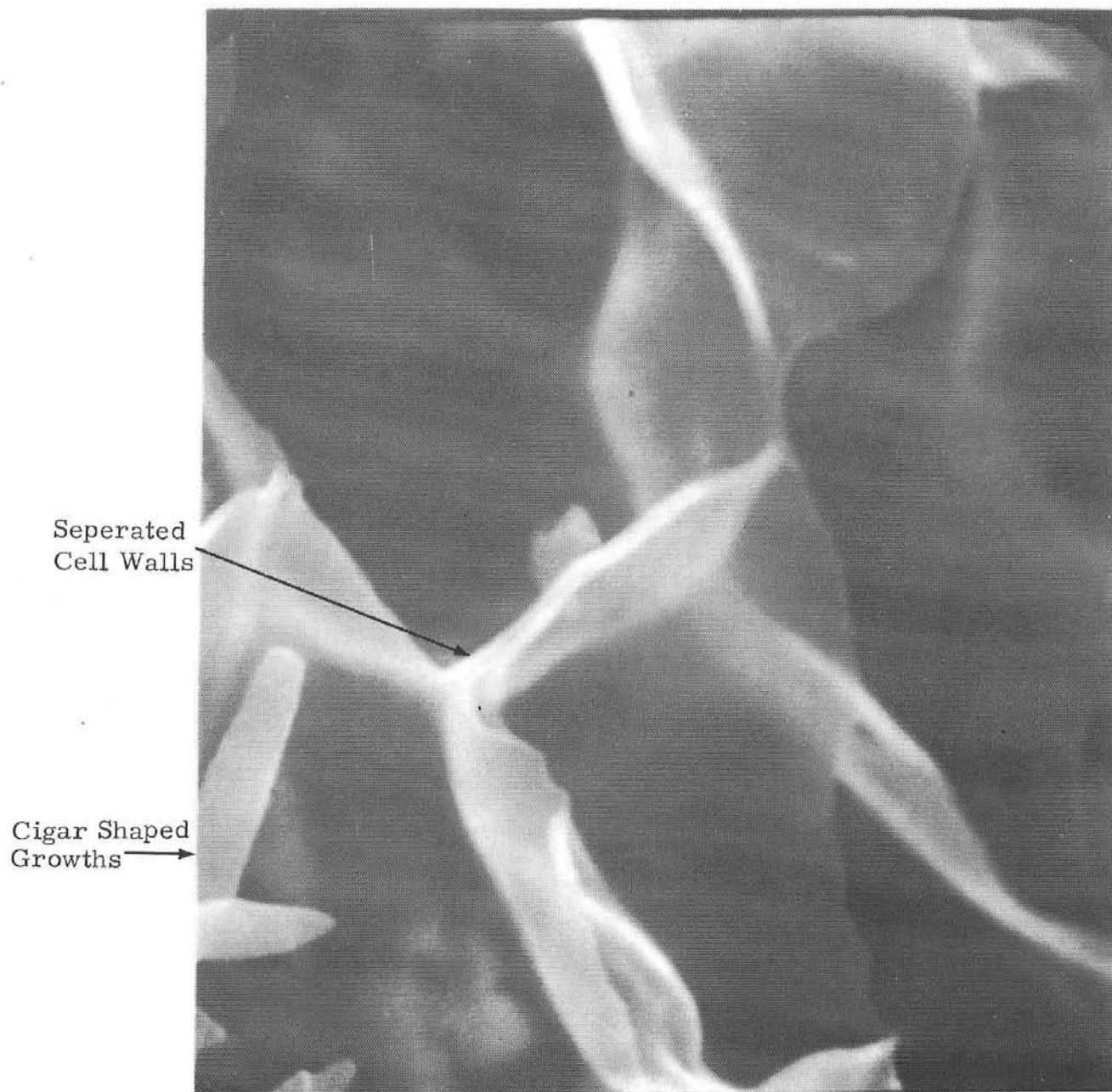


Figure 15. TKD graphitized at 3000°C showing a rare wall separation and cigar shaped growths.

The higher density of the composition cork was caused by the addition of a phenolic adhesive. Figure 3 shows an envelope of approximate TKD cell sizes as a function of density. Cell sizes are small enough to block radiation heat transfer over the entire density range.

Figure 16 shows a section of high density graphite TKD made from composition cork with a phenolic binder. This micrograph was taken at a granule boundary and shows an area with completely collapsed cells where there was apparently a projection on one of the particles. Some areas of local cell collapse can be found in all composition corks, but it is more prevalent in the higher densities. The degree of cell distortion is usually larger along granule boundaries than in the center of the granules. Also shown in Figure 16 are the carbonized phenolic adhesive between granules and a cluster of cigar shaped growths. All cells are more flattened than those in the lower density TKD shown in Figure 12.

When cork is heated during the formation of corkboard or isolation cork, the cells flow slightly, which allows the voids between granules to be filled with a minimum of cell collapse. This is illustrated in Figure 17 which shows the boundary area in high density TKD made from isolation cork. Granules are held together by carbonized lignin which came from the cork granules.

A fracture surface of 13.3 lb/ft graphitized corkboard is shown in Figure 18. The fracture followed granule boundaries, which was the case for all TKD insulations that did not have adhesive added to the cork composite precursors. Fracture planes in TKD made from composition cork, such as that shown in Figure 16, did not follow granule boundaries.

Thermal Conductivity Tests

The conductivities of carbon and graphite TKD were measured at Union Carbide's Parma Technical Center using the cyclic temperature phase shift technique in one atmosphere of argon and at Sandia Laboratories using the laser pulse technique in a vacuum. Tests were conducted on TKD's made from 30 lb/ft³ composition cork with 16/50 size granules and a phenolic binder, 21 lb/ft³ isolation cork with 6/30 size low grade ground cork and no added binder, and 14.5 lb/ft³ corkboard with 20/40 size granules and no added binder. The results of the tests are given in Table V.

The tests results are also shown graphically in Figures 19 and 20. The larger change in graphite TKD conductivity with density than in carbon TKD is partially due to the larger percent of heat that is transferred by solid conduction in the graphite form. There is a small disagreement between data obtained in the two facilities, but this is common because of the difficulties in measuring the conductivity of insulators at high temperatures. The conductivities of both carbon and graphite TKD are close to the predicted values from Reference 9 (Figures 21 and 22). The conductivities of these insulations are governed primarily by the conductivity of the solid walls. Radiation heat transfer is negligible even at high temperatures. The conductivity of graphite TKD actually decreases at high temperatures following the shape of the graphite conductivity curve (Figure 2). The lower than predicted conductivity at low temperatures is probably caused by incomplete graphitization and carbonization.

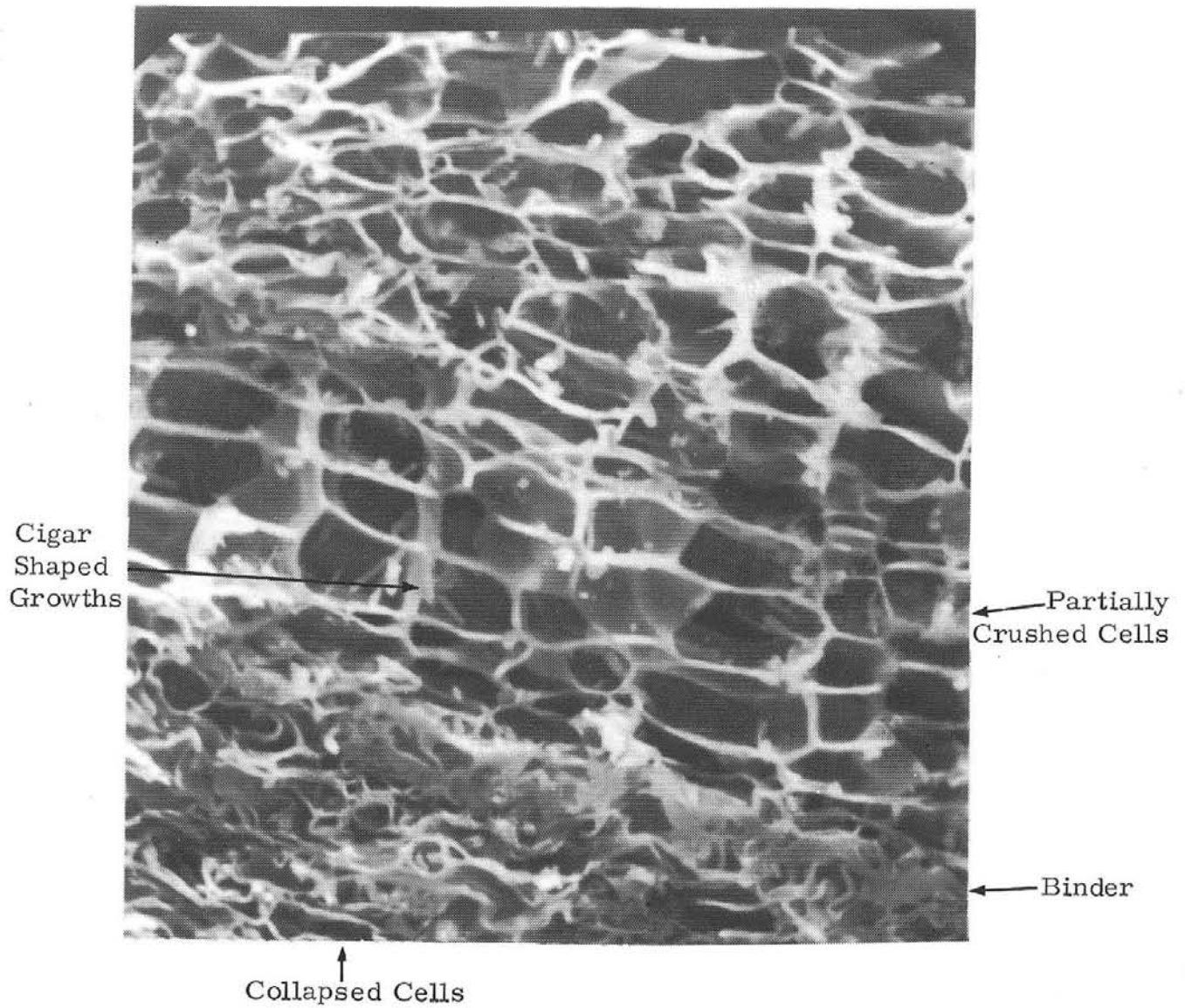
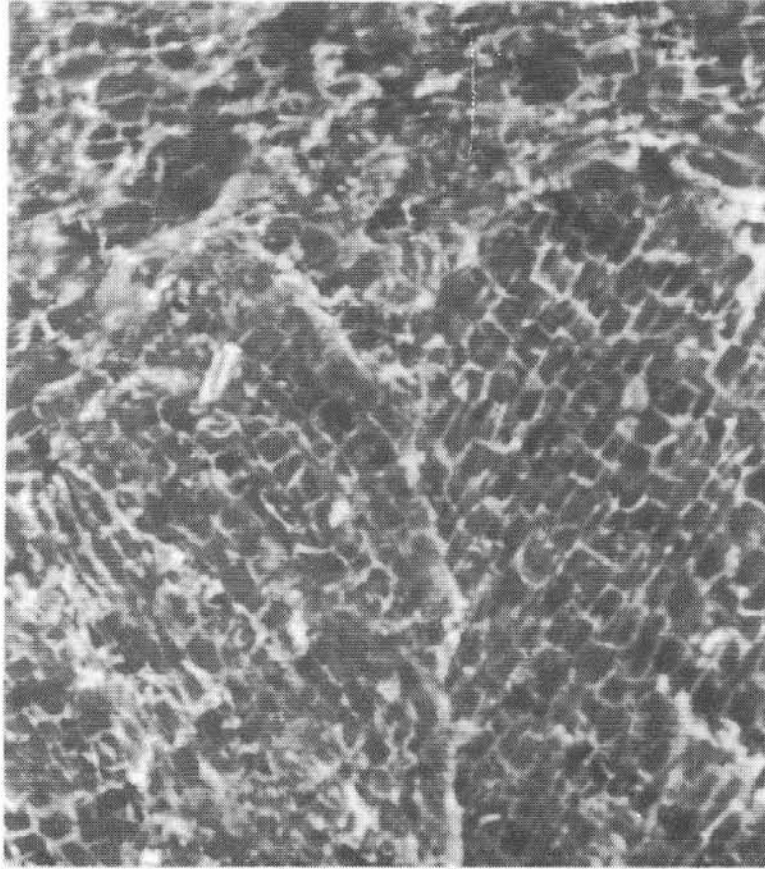


Figure 16. Graphitized 29.5 lb/ft³ composition cork with phenolic binder showing cell distortion and local cell collapse at a granule boundary.



Granule Boundary

Figure 17. Cut surface of carbonized isolation cork.

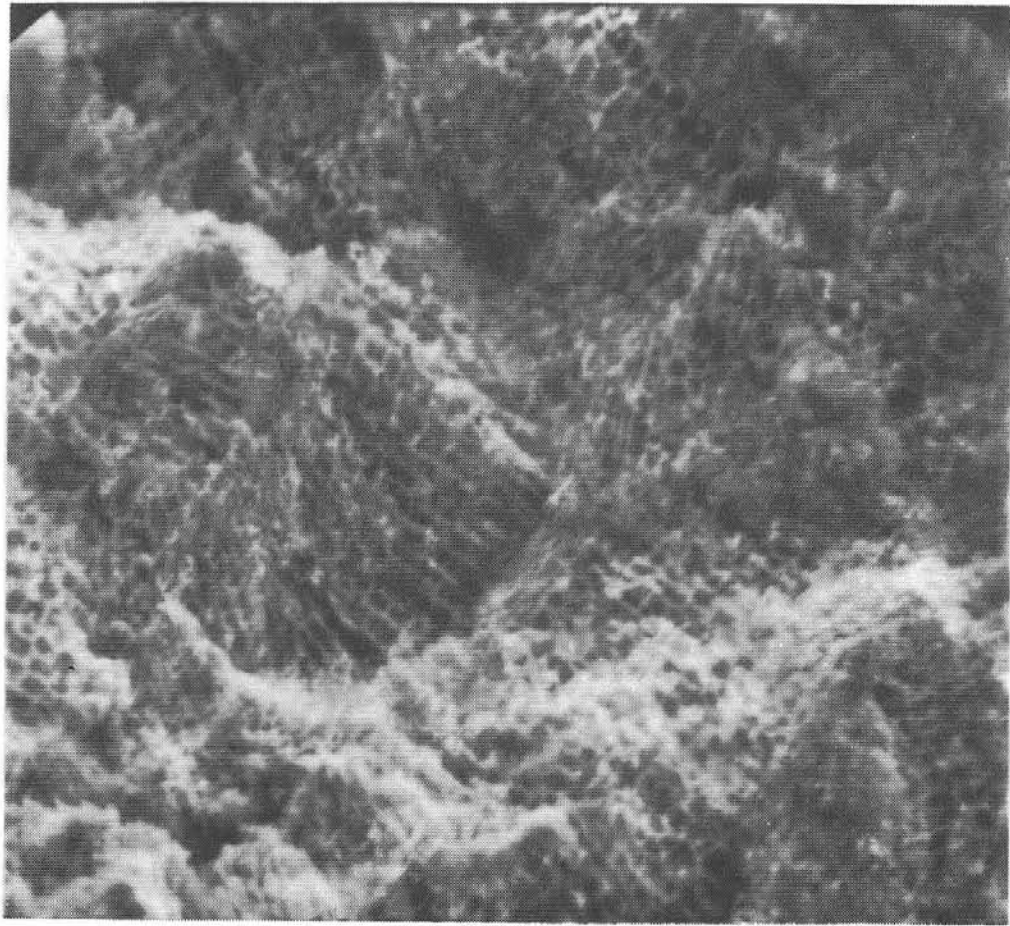


Figure 18. Fractured surface of graphitized corkboard.

TABLE V

Thermal Conductivities of Several Carbon
and Graphite TKD Insulations

Atmosphere	Temp. ($^{\circ}\text{C}$)	Temp. ($^{\circ}\text{R}$)	Conductivity (Btu/Hr Ft $^{\circ}\text{R}$)
<u>Precursor</u> 30 lb/ft 3 16/50 Phenolic Cork			
<u>Carbonized</u> $\rho = 24.5$ lb/ft 3			
Argon	1316	2860	0.358
Vacuum	554	1489	0.121
	777	1890	0.169
	1154	2569	0.416
	1530	3245	0.600
	1730	3605	0.980
<u>Graphitized</u> $\rho = 29.5$ lb/ft 3			
Argon	1300	2833	1.166
	1903	3919	1.345
	2244	4532	1.372
	2304	4639	1.318
	2390	4793	1.379
	2522	5033	1.243
Vacuum	554	1489	1.135
	777	1890	1.178
	1154	2569	1.389
	1530	3245	1.514
	1730	3605	1.589
<u>Precursor</u> 21 lb/ft 3 Isolation Cork			
<u>Carbonized</u> $\rho = 13.5$ lb/ft 3			
Vacuum	537	1458	0.156
	749	1840	0.173
	1070	2419	0.232
	1349	2920	0.373
	1954	4009	0.842
<u>Graphitized</u> $\rho = 17.5$ lb/ft 3			
Vacuum	515	1418	0.781
	892	2099	0.841
	1242	2729	0.934
	1537	3258	1.106
	1982	4059	1.071
<u>Precursor</u> 14.5 lb/ft 3 20/40 Corkboard			
<u>Graphitized</u> $\rho = 13.3$ lb/ft 3			
Vacuum	523	1433	0.512
	920	2149	0.592
	1303	2839	0.676
	1616	3400	0.729
	2120	4309	0.841

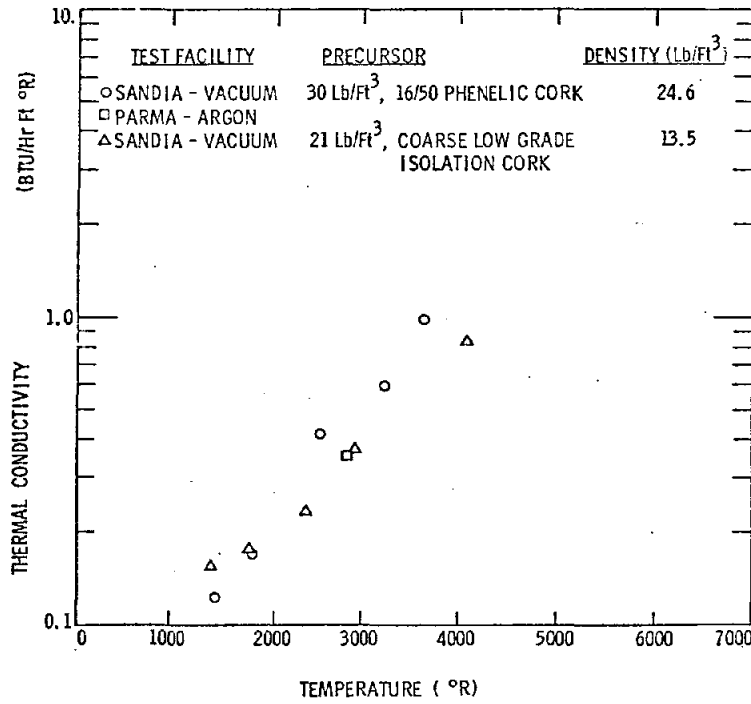


Figure 19.
Thermal conductivity of graphitized composition cork.

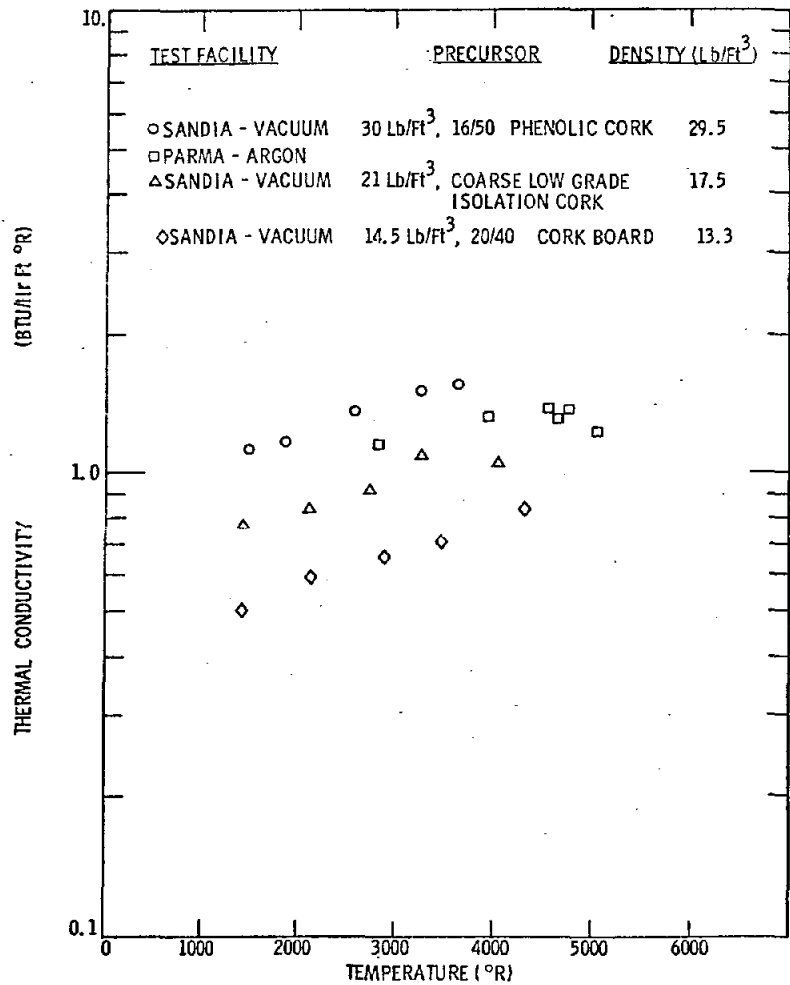


Figure 20.
Thermal conductivity of carbonized composition cork.

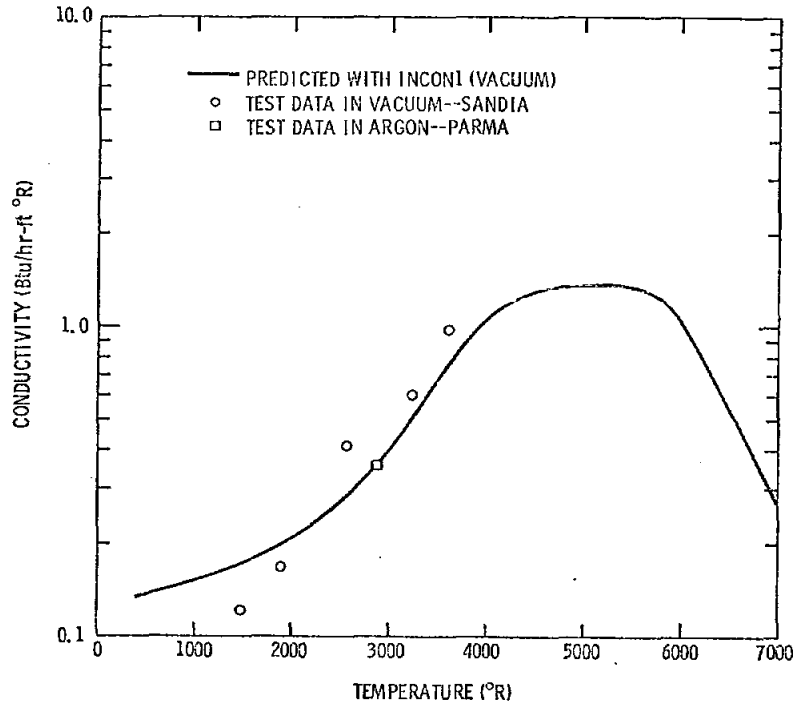


Figure 21. Thermal conductivity of carbonized phenolic cork. $\rho = 24.6 \text{ lb/ft}^3$. Crushed parallel to heat flow, $Y = 0.8$.

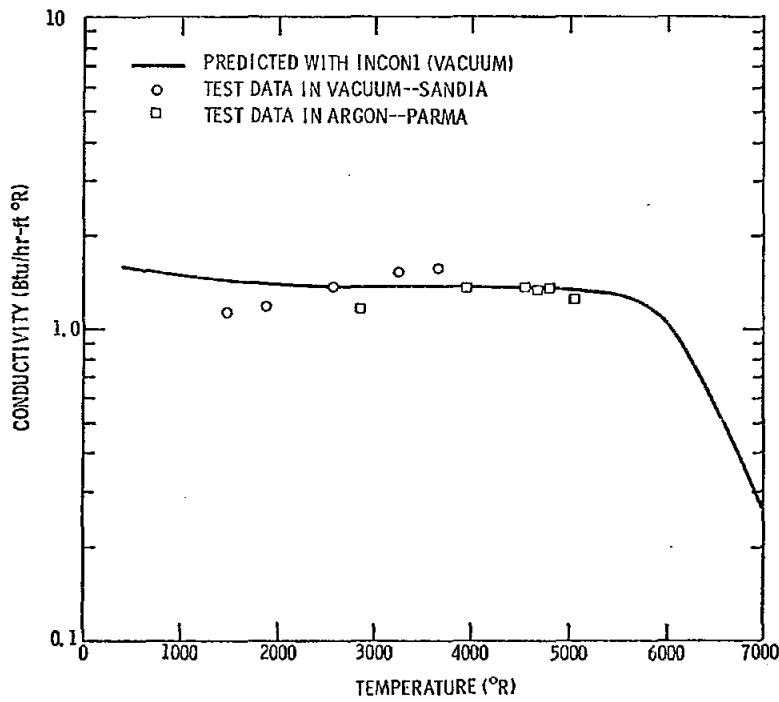


Figure 22. Thermal conductivity of graphitized phenolic cork. $\rho = 29.5 \text{ lb/ft}^3$. Crushed parallel to heat flow, $Y = 0.8$.

Figure 23 shows a comparison between TKD and some of the most efficient carbon foams and fibrous carbon high temperature insulations made by several manufacturers (Ref. 21). The conductivity of carbon TKD is lower than that of carbon foams for all temperatures. The conductivity of carbon TKD at low temperatures would be about the same as a fibrous carbon of the same density. At temperatures above 4000°R, the conductivity of carbon foam and fibrous carbon increases proportionally to temperature cubed because of radiation heat transfer (Ref. 5), but the rate of increase for carbon TKD decreases with temperature. The conductivity of graphite TKD is nearly constant, and at high temperatures it has a lower conductivity than foam or fibrous carbon.

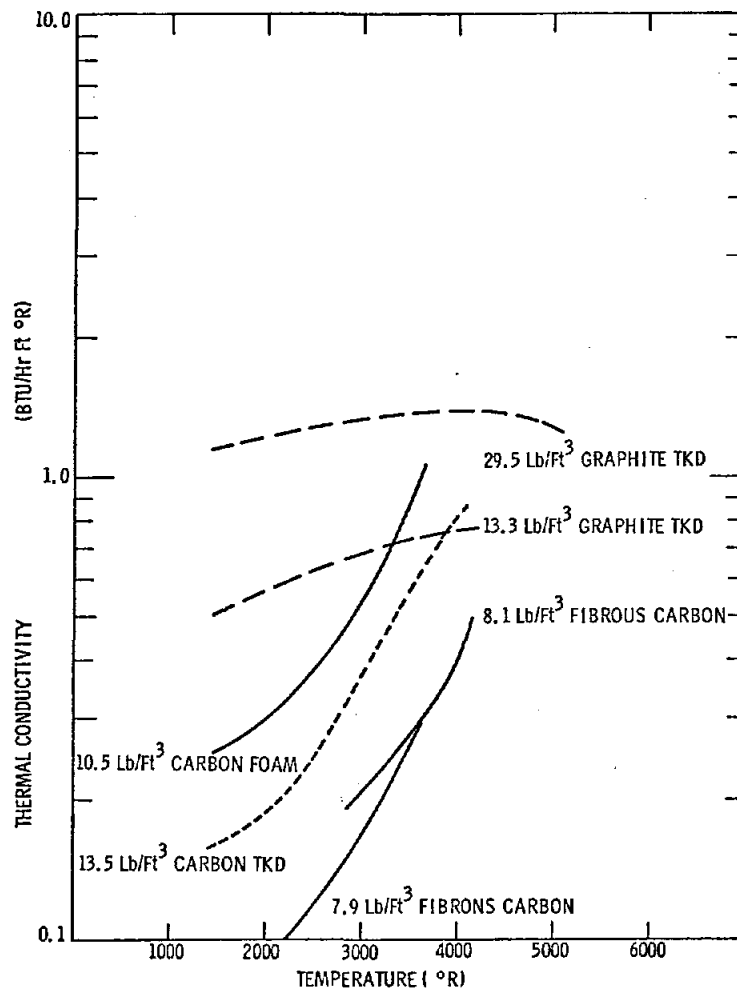


Figure 23. Thermal conductivity comparison of TKD, carbon foam, and fibrous carbon.

Electrical resistivity can be used to measure the effective cross section area divided by the path length for solid conduction and to locate discontinuities which are perpendicular to heat flow. Table VI compares the resistivities of carbon and graphite with TKD insulations.

TABLE VI

Average Electrical Resistivities
of Carbon, Graphite, and TKD

<u>Material</u>	<u>Resistivity (Ohm - m)</u>
Carbon	3.6×10^{-5}
13.5 lb/ft ³ Carbon TKD	2.0×10^{-3}
Graphite	9.0×10^{-6}
17.5 lb/ft ³ Graphite TKD	5.0×10^{-4}

The TKD's in Table VI were made from low grade isolation cork with no binder added. Comparison of measured resistivities with those computed from known cell configurations indicates that there were some discontinuities or high contact resistances at granule boundaries.

Mechanical Tests

Room temperature mechanical properties of TKD were measured and compared to those of foam and fiber insulations. A typical compression stress/strain curve for TKD is shown in Figure 24. Elastic deformation is nearly linear and ranges from 0.66 percent for carbonized isolation cork to 1.32 percent for graphitized composition cork. Failure begins with crushing of the surface cells. When only surface cells are failing, the maximum stresses vary, but the average remains nearly constant. At about 6 percent compression, internal failures, primarily at granule boundaries, begin to occur, and the failure stress level begins to decrease.

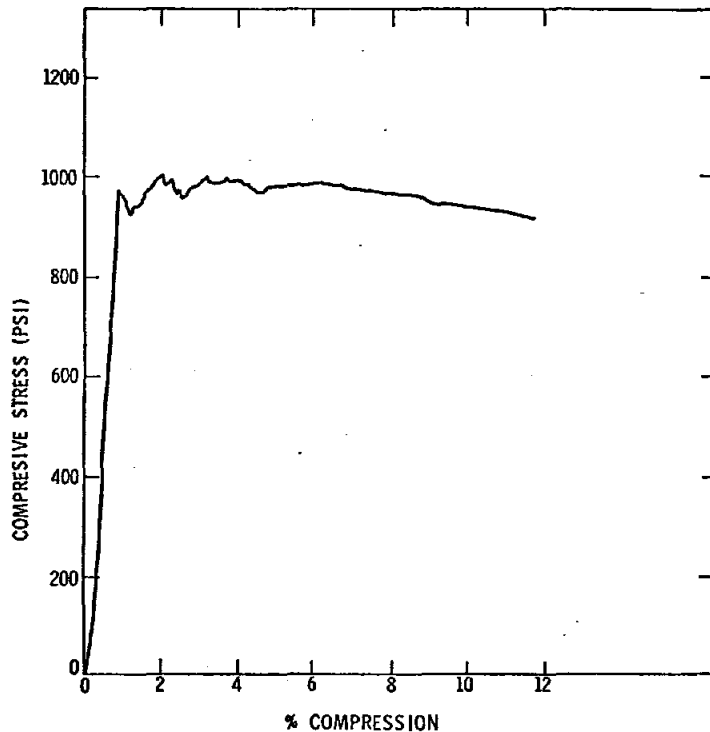


Figure 24. Compressive stress/strain curve for 24.5 lb/ft³ carbon TKD insulation.

Compression properties for several carbon and graphite insulations are listed in Table VII. All tests were made with non-bonded surfaces and no initial surface crushing. The strengths of the TKD insulations are between those of the foams and fibrous insulations. Rigidity is about the same as the foams. The properties of TKD had good repeatability with crush stress and elastic elongation being ± 1.5 percent for the graphite forms and ± 4.0 percent for the carbon forms.

TABLE VII
Comparison of Compressive Strengths
Of TKD, Carbon Foam, and Fibrous Carbon

Material	Density (lb/ft ³)	Crush Stress (psi)	Stress at 10% Deflection (psi)	Stress at 20% Deflection (psi)	Modules of Elasticity (psi)	% Compression When Crushing Begins
Fibrous Carbon	8.2	-	24	35	384	-
Fibrous Carbon	14.9	-	171	245	3,610	-
Carbon Foam	12.5	876	-	-	71,300	0.81
Carbon TKD (Isolation Cork Precursor)	13.5	593	-	-	91,500	0.66
Carbon TKD (Composition Cork Precursor)	24.6	960	-	-	107,600	0.89
Graphite TKD (Isolation Cork Precursor)	17.5	339	-	-	44,000	0.80
Graphite TKD (Composition Cork Precursor)	29.5	596	-	-	45,000	1.32

Tensile strength of 13.5 lb/ft³ carbon TKD was 238 psi compared to 230 psi for 12.5 lb/ft³ carbon foam.

All of the properties of TKD insulations given in this section were for experimental compositions and processes. Optimization should improve and broaden the range of properties.

Fiber Reinforced TKD

Cellular materials such as TKD and polyurethane based carbon foams are usually weak in tension as shown in Reference 21 and in the Mechanical Tests section of this report. One method of increasing the tensile strength of a material is by the addition of fibers. When used in a cellular insulation, the fibers must mix uniformly, must adhere to the matrix material, and must not form voids. In addition, if the cells and fibers are carbonized, the shrinkage of the two materials must be equal so the fibers will not buckle or pull free of the matrix.

The linear shrinkage of cork during carbonization is 27 to 30 percent. Rayon is the most similar fiber with a shrinkage of 27.5 to 31.9 percent (Ref. 22). Fine fibers should be used for better homogeneity and to allow the fibers to follow granule boundaries for better keying, fewer voids, and less cell deformation. The fibers should be at least as long as 6 to 10 granules to insure good keying and span enough cork to increase strength.

A reinforced corkboard was fabricated with 7.5 percent rayon by weight, which was 1.2 percent by volume. The fiber diameters were 0.0011 inch, and lengths were about 0.3 inch. The fibers were crimped, which caused them to felt and mix poorly with the cork granules. Straight fibers have been found to mix more easily and more uniformly. Initial orientation of the fibers in the matrix was random, but when the mixture was compressed during the formation of corkboard, a preferential orientation developed normal to the direction of compression.

The reinforced corkboard was carbonized with a 50-hour cycle having a maximum temperature of 1000°C. Linear shrinkage was 27 percent. No evidence of differential shrinkage between fibers and the cork granules could be found in electron micrographs. Figures 25 and 26 are micrographs of two tensile fractures. All fractures occurred along granule boundaries, indicating there was insufficient lignin to bond both the granules and the added fibers. There was also little evidence of bonding between the fibers and cork. Fibers were secured primarily by keying (Figure 25). When the fracture occurred near the end of the fiber, the fiber pulled out (Figure 25), but when the fracture was near the middle of the fiber, the fiber fractured (Figure 26). Greater strength should be obtained if lignin coated fibers are used or if a small amount of lignin is added to the mixture to compensate for the increased surface area and small gaps around some of the fibers. Figure 26 shows some of the nonhomogeneity caused by felting of the fibers and the cell distortion around the fibers. Longer and finer straight fibers should increase strength and reduce voids and crushing. More fibers could also be added to increase strength.

Table VIII compares the tensile strength of carbon foam, carbon TKD, and reinforced TKD. Even though the reinforcing was far from optimized, the addition of 1.2 percent fibers by volume increased strength by 18 percent.

Polyurethane foam and PAN acrylic fibers also have approximately the same shrinkage during carbonization. If acrylic fibers can be foamed uniformly in place, the result could be stronger polyurethane and carbon foams. This combination has not as yet been fabricated.

TABLE VIII
Comparative Tensile Strength
Of TKD and Carbon Foam

<u>Material</u>	<u>Density (lb/ft³)</u>	<u>Tensile Strength (lb/in²)</u>
Carbon Foam	12.5	230
Carbon TKD	13.5	238
Carbon TKD with 1.2% Fibers	13.3	281

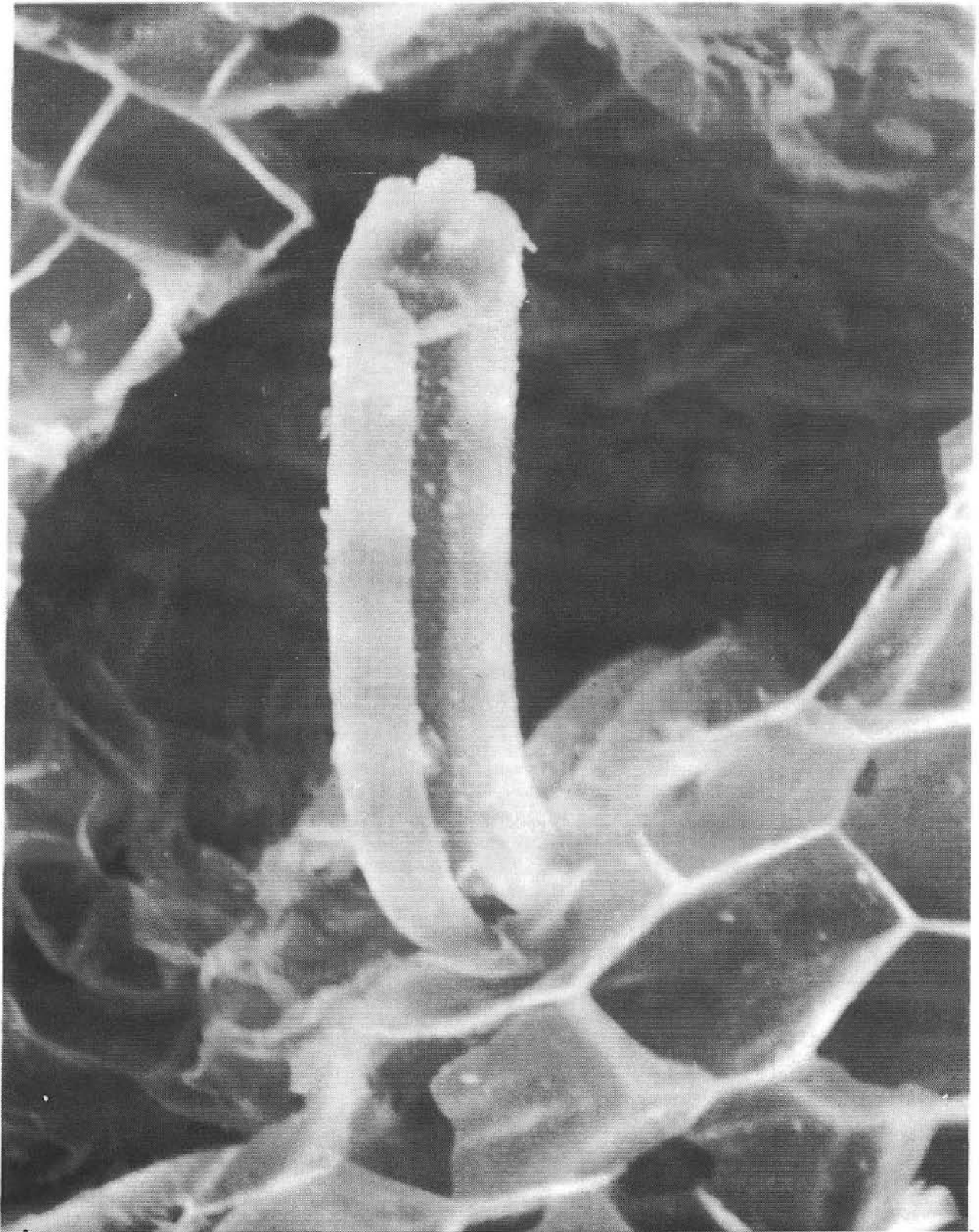


Figure 25. Tensile fracture of reinforced carbon TKD showing fiber keying and a granule pull out.

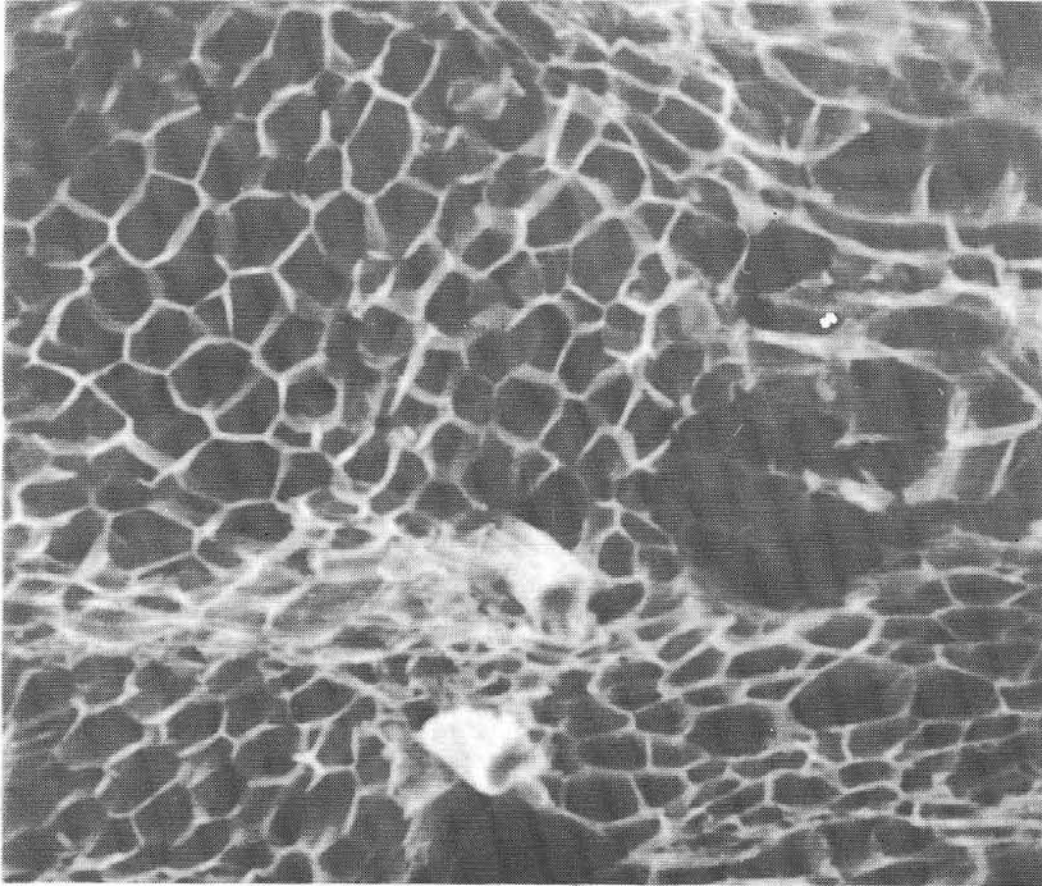


Figure 26. Local cell crushing around reinforcing fibers.

Applications

TKD was originally designed as reentry insulation around heat sources in radioisotopic thermoelectric generators (RTG's) used in the space program. In this application, the temperature dependence of conductivity is as important as a low value of conductivity because heat must be rejected through the insulation at the relatively low operating temperatures of the generators but the heat flow must be limited during reentry at higher temperatures. The conductivity of graphite TKD does not increase with temperature, it is strong enough to support a heat source in an RTG and it is resilient enough to compensate for thermal expansion.

Other potential uses for carbon or graphite TKD include the following.

1. Load bearing insulation behind high conductivity ablation shields on reentry vehicle bodies and control surfaces. Since TKD is rigid and is closed celled, it may be possible to filament wind over the insulation and carbon vapor deposit (CVD) the entire unit to form a one-piece ablation/insulation structure similar to the RFD-1 reentry vehicle (Ref. 12).
2. Space vehicles returning from super-orbital missions can make several high altitude passes through the earth's atmosphere before the final reentry (Ref. 4). These passes are usually in free molecule or transition flow where heating rates are relatively low and the ablation material is inefficient. The result is a preheating of the ablation material and structure before the final high heating rate reentry. A two layer ablation system consisting of an insulator/ablator over the conventional ablation material may reduce the preheat problem. TKD should be well suited for the outer layer because heat could be re-radiated from a high temperature surface while heat flow inward would be retarded. Strength should be adequate for the low forces in free molecule flow. The outer layer would ablate off rapidly when continuous flow is reached.
3. Wake areas of reentry vehicles can have high enough heating rates to require refractory insulator/ablaters. Some low ballistic coefficient R/V's can survive with polymer insulations in wake and separated flow areas, but high performance R/V's need higher temperature insulation such as TKD.
4. As an insulator for planetary probes where temperatures exceed 5000^oR.
5. High temperature insulation on any apparatus in a vacuum, inert atmosphere, or confined atmosphere.
6. Applications requiring a minimal change in conductivity with temperature.

Conclusions and Recommendations

The development of TKD was primarily analytical. Tests were used only to evaluate the design and to characterize the properties. The only precursors tested were composition corks, and only high carbon yield adhesives were used to bond granules together. All the precursors are inexpensive and processing costs are comparable to other carbons and graphites. Precursors can be formed to any desired shape, and TKD is easily machined at any stage of processing. There has been no optimization of TKD, but tests have indicated how improvements can be made. Even though the TKD insulations have not been perfected, tests showed that mechanical properties are nearly as good as the strongest high temperature insulators, and at temperatures above 4500^oR TKD has a lower conductivity than any porous insulator tested. The conductivity of graphite TKD is nearly constant from room temperature to 5100^oR. The structure of TKD is uniform across thick sections, and structure, mechanical properties, and thermal conductivity have excellent repeatability.

Further development of TKD should improve mechanical properties, reduce and extend range of thermal conductivities, improve carbon yield, and provide more complete thermo-physical property data. Specific areas in need of development are the following.

Precursors

The density range of the precursors and hence the density range of TKD can be extended by changing the curing temperature and pressure, by using expanded cork, and by changing adhesive types and quantities. Radiation heat transfer is small enough to permit the cells to be enlarged without a significant increase in high temperature conductivity. Adhesives added to cork granules to form composition cork should have high fluidity before curing and have the same shrinkage and yield during carbonization as cork. Lignin, the natural binder in cork, and some phenolics appear to produce the best bonding with the smallest amount of added material. The lowest density cork boards are made without added binder. Since cork flows slightly and the cells expand when heated, a more uniform precursor with fewer voids should result from a longer high temperature cure with compression forces applied at high temperature before the adhesive cures.

The tensile strength of reinforced TKD could be improved by using longer and finer straight rayon fibers in the precursor. An adhesive is needed to make full use of the added strength of the fibers. The maximum fiber constant has not been determined.

Carbonization and Graphitization

Carbonization was found to be nearly complete at 1100^oC, but graphitization was not complete at 3000^oC. A higher temperature cycle is needed to completely graphitize TKD. The carbon yield was higher at one atmosphere pressure than when the cork was carbonized in a vacuum. A pressurized cycle may increase the carbon yield and reduce shrinkage even further. Catalysts have been used to increase carbon yields and enhance graphitization at lower temperatures. Catalysts may also be used to improve TKD.

Tests

The composition of the gas in the closed TKD cell is not known. Initially the gas is air, but it is at least partially displaced by nitrogen and carbon dioxide during carbonization. Diffusion rates through TKD are also not known. Tests must be run to measure evacuation rates and the time required for TKD cells to reach equilibrium with a surrounding gas. Diffusion rates are also needed to determine if there are any practical limits on maximum rates of temperature or pressure change.

Combined insulation/ablation tests are needed to measure the efficiency of TKD for reentry vehicle wake area and free molecule flow thermal protection. A simple test simulating flow impinging surfaces at high altitudes could be conducted in some low density plasma jet facilities using the method described in Reference 23. Wake heating can be simulated with radiant heaters, as described in Reference 13. Laser and X-ray tests can measure the high density, short pulse, energy absorbing capabilities of TKD.

After the formulations of TKD are finalized, more complete characterization tests will be needed, including: compressive, tensile, and flexure strength and modulus of elasticity; conductivity; thermal expansion; specific heat; and emittance.

Although TKD could be used in its present form, further development should increase its efficiency and extend its usage.

References

1. R. D. Klett, Thermal Design of a Snap-19 Generator for Intact Reentry (U), SC-RR-67-197, Sandia Laboratories, Albuquerque, NM, May 1967, (CRD).
2. R. D. Klett, Design of Space Nuclear Power Supplies for Intact Reentry, SC-RR-68-351, Sandia Laboratories, Albuquerque, NM, May 1968.
3. R. D. Klett, Thermal Design and Analysis of the Apollo Lunar Radioisotopic Heater, SC-RR-71-0533, Sandia Laboratories, Albuquerque, NM, September 1971.
4. R. D. Klett, Pioneer Heat Source Aerothermodynamic Analysis: Volume III - Aeroheating, Ablation, and Design Modifications, SC-RR-71-0168, Sandia Laboratories, Albuquerque, NM, May 1971.
5. R. U. Acton and G. F. Wright, Properties of Carbon Thermal Insulation, SC-TM-69-80, Sandia Laboratories, Albuquerque, NM, February 1969.
6. C. L. Mantell, "Carbon and Graphite Handbook," Interscience Pub., New York, 1968.
7. Y. S. Touloukian, "Thermophysical Properties of High Temperature Solid Materials," Vol. I, MacMillan, New York, 1967.
8. W. N. Reynolds, "Physical Properties of Graphite," Elsevier Pub. Co., New York, 1968.
9. R. D. Klett, Analytical Thermal Design of Cellular Insulations and Laminated Composites, SAND-74-0232, Sandia Laboratories, Albuquerque, NM, January 1975.
10. J. Corll, Concerning the High Temperature Thermal Conductivity of Carbon Foams, SC-RR-70-622, Sandia Laboratories, Albuquerque, NM, September 1970.
11. R. W. Hovey, "Cork Thermal Protection Design Data for Aerospace Vehicle Ascent Flight," AIAA Paper No. 64-356, July 1964.
12. R. E. Berry, S. L. Jeffers, R. D. Klett, et al., Final Report on Reentry Flight Demonstration Number Two - Reentry Systems Description Section, SC-RR-65-43, Sandia Laboratories, Albuquerque, NM, April 8, 1965.
13. R. D. Klett, Design and Testing of Ablation Systems for Low Heating Rate and Low Shear Force Applications, SC-RR-66-35, Sandia Laboratories, Albuquerque, NM, April 1966.
14. Kirk and Othmer, "Encyclopedia of Chemical Technology," Vols. 6 and 12, Interscience Pub., New York, 1965.
15. S. L. Madorsky, "Thermal Degradation of Organic Polymers," Interscience Pub., New York, 1964.
16. N. O. V. Somtag, Fatty Acids, "Dehydration, Pyrolysis, and Polymerization", Interscience Publications, Inc., New York, New York, 1961.
17. H. A. Mackay, The Conversion of Synthetic Resins to Amorphous Carbon, SC-RR-68-296, Sandia Laboratories, Albuquerque, NM, July 1969.
18. "Thomas Register of American Manufacturers and Thomas Register File 1972 - Vol. 2," Thomas Pub. Co., New York, 1972.
19. "Armstrong Ablation Material-Insulcork 2755," Armstrong Cork Co. Catalog, Lancaster, Pa. 1963.

References (cont)

20. M. L. Lieberman, C. R. Hills, and C. J. Miglionico, "Growth of Graphite Filaments," *Carbon*, 1971, Vol. 9, pp 633.
21. L. G. Rainhart and E. R. Frye, Development of Carbon Thermal Insulation for the Materials Test Vehicle (MTV-1) Program, SC-DR-70-924, Sandia Laboratories, Albuquerque, NM, April 1971.
22. H. O. Pierson and J. F. Smatana, Carbonization of Rayon Felt, SC-TM-68-255, Sandia Laboratories, Albuquerque, NM, May 1968.
23. R. D. Klett, Ablation Material Testing, SC-RR-68-601, Sandia Laboratories, Albuquerque, NM, December 1968.

DISTRIBUTION:

TID-4500-R62-UC25 (213)

U. S. ERDA (5)

Division of Space Nuclear Systems
Washington, DC 20545
Attn: David S. Gabriel (1)
George P. Dix (2)
Harold Jaffe (2)

U. S. ERDA (2)

Albuquerque Operations Office
Special Programs Division
P. O. Box 5400
Albuquerque, NM 87115
Attn: Duard K. Nowlin
Dennis L. Krenz

U. S. ERDA

Division of Controlled Thermonuclear Research
Washington, DC 20545
Attn: Dr. R. L. Hirsch

U. S. ERDA (2)

Division of Military Applications
Washington, DC 20545
Attn: Major General Ernest Graves, USA
Cmdr. Wayne Beech, USN

U. S. ERDA

Division of Naval Reactors
Washington, DC 20545
Attn: H. F. Raab (NC)

U. S. ERDA

Division of Nuclear Materials Security
Washington, DC 20545
Attn: Samuel C. T. McDowell

U. S. ERDA

Operational Safety
Washington, DC 20545
Attn: Robert E. Yoder

U. S. ERDA

Division of Physical Research
Washington, DC 20545
Attn: Dr. D. K. Stevens

U. S. ERDA (3)

Division of Reactor Research and Development
Washington, DC 20545
Attn: Merrill J. Whitman
George W. Cunningham
William Hannum

U. S. ERDA (2)

Division of Waste Management and Transportation
Washington, DC 20545
Attn: Robert W. Ramsey, Jr.
Owen P. Gormley

U. S. ERDA (4)

Division of Reactor Safety Research
Washington, DC 20545
Attn: Dr. Herbert J. C. Kouts
William H. Layman
Dr. Long Sun Tong
Dr. Charles N. Kelber

U. S. ERDA

Albuquerque Operations Office
Patents Division
P. O. Box 5400
Albuquerque, NM 87115
Attn: Ignacio Resendez

Gulf General Atomic, Incorporated
P. O. Box 1111

San Diego, CA 92112

Attn: N. B. Elsner, Chief
Technical Information Services

Jet Propulsion Laboratory (2)

California Institute of Technology
4800 Oak Grove Drive
Pasadena, CA 91103
Attn: R. G. Ivanoff, (277-102)
V. Truscillo, (277-102)

Massachusetts Institute of Technology (3)

Lincoln Laboratory
P. O. Box 73
Lexington, MA 02173
Attn: R. Matlin
Dr. A. Stanley
P. Waldron

Los Alamos Scientific Laboratory (4)

P. O. Box 1663
Los Alamos, NM 87455
Attn: R. Baker, SM-29
R. B. Duffield, TA-46
H. T. Motz, SM-40
W. A. Ranken, TA-46

Radio Corporation of America (2)

Electronic Components
415 South 5th Street
Harrison, New Jersey 07029
Attn: L. Caprarola
G. Silverman

Minnesota Mining & Manufacturing Co.

2501 Hudson Road
St. Paul, Minnesota 55119
Attn: E. Hampl

Battelle Memorial Institute (2)

Columbus Laboratories
505 King Avenue
Columbus, Ohio 43201
Attn: W. Pardue
N. Proberskin

DISTRIBUTION (cont):

Atomics International
Division of North American Aviation, Inc.
P. O. Box 309
Canoga Park, California 91305
Attn: N. Miller

Isotopes, Inc.
Nuclear Systems Division
110 West Timonium Road
Timonium, Maryland 21093
Attn: W. W. Wachtl

TRW Systems Group
One Space Park
Redondo Beach, California 92078
Attn: M. W. Novick

Fairchild Industries
Space & Electronics Division
Germantown, Maryland 20767
Attn: Al Schock

Syncal Corporation
430 Persian Drive
Sunnyvale, California 94086
Attn: Mr. Valvo Ragg

General Electric Company
Missile and Space Division
Vally Forge, Pa. 19101
Attn: Richard Katucki

Union Carbide Corporation
Linde Division, Engr'g Department
61 West Park Drive
Tonawanda, New York 14150
Attn: F. Notaro, Supervisor
New Products Development Engineering

The Boeing Company
Aerospace Group
P. O. Box 3999
Seattle, Washington 98124
Attn: Hugh D. Boring M.S. 8C-31
Grand Tour Program Manager

National Aeronautics & Space Administration (2)
Headquarters
Washington, D. C. 20546
Attn: W. Keller (Code SL)
T. B. Kerr (Code RY) Assistant
Director Nuclear Safety, Room B-556

National Aeronautics & Space Administration (4)
Lewis Research Center
21000 Brookpark Road
Cleveland, Ohio 44135
Attn: R. Titran/M.S. 105-1
C. S. Corcoran/M.S. 500-202
W. J. Bifano/M.S. 302-1
R. E. English/M.S. 500-201

National Aeronautics & Space Administration (2)
Langley Research Center
Langley Station
Hamptom, Virginia 23365
Attn: Dr. R. Trimpi
R. A. Russell/M.S. 159

National Aeronautics & Space Administration (2)
Ames Research Center
Moffett Field, California 94035
Attn: H. K. Larson, MS 234-1
A. C. Wilbur/DES

National Aeronautics & Space Administration
Manned Spacecraft Center
Houston, Texas 77058
Attn: J. Briley - ET - 5

National Aeronautics & Space Administration
George C. Marshall Space Flight Center
Marshall Space Flight Center, Alabama 35812
Attn: R. Rood - PD-DO-EP

Oak Ridge National Laboratory (2)
U. S. Atomic Energy Commission
P. O Box X
Oak Ridge, Tenn. 37830
Attn: Eugene Lamb, Asst. Superintendent
Isotopes Division
R. G. Donnelly

Aerospace Corporation (4)
P. O. Box 92957
Worldway Postal Center
Los Angeles, Calif. 90009
Attn: R. G. Allen
R. A. Hartunian
D. T. Nowlan
W. M. Mann, Jr.

TRW Systems Group
One Space Park
Redondo Beach, California 90278
Attn: Herman S. Heaton
For: P. O. Finnie (1)

SAMSO (RSA) (5)
P. O. Box 92960
Worldway Postal Center
Los Angeles, Calif. 90009
For: Col. Howard M. Estes (1)
Col. A. Aharonian (1)
Lt. Col. C. R. Hutchinson (1)
Attn: Capt. W. G. Williams
Col. D. Dowler (1)
Lt. Col. Gilbert (1)

DISTRIBUTION (cont):

McDonnell Douglas Corporation
Astronautic Company
5301 Bolsa Avenue
Huntington Beach, Calif. 92647
Attn: Norman Stanley Beer
For: Mr. Ken Kretsch (1)

U. S. Army Advanced Ballistic Missile
Defence Agency
The Commonwealth Building
1300 Wilson Blvd.
Arlington, Virginia 22200
Attn: Jacob B. Gilstein (1)

Hq. USAF (RDCCO) (2)
DCS/Research and Development
Washington, D. C. 20330
Attn: Division Chief, AF/RDQPN
For: Dr. W. L. Lehmann (1)
Maj. J. G. Burton (1)

Document Control Officer
DARD-AOA-M, Dept. of the Army
Room 3D-442, The Pentagon
Washington, D. C. 20310
Attn: Maj. Gen. William C. Gribble, Jr. (1)

Director, Defense Nuclear Agency (2)
Washington, D. C. 20305
Attn: Chief, Administrative Service Branch
For: J. F. Moulton, Jr. (1)
Maj. R. E. Jackson (1)

Dr. Malcolm R. Curri
Director of Defense Research & Engineering (2)
Room 3E1006, The Pentagon
Washington, D. C. 20301
Attn: J. Persh (1)
G. R. Barse (1)

Defense Advance Research Projects Agency
1400 Wilson Blvd.
Arlington, Virginia 22209
Attn: Fred A. Koether
For: Dep. Dir., ARPA (1)
Defense Research & Engineering

Director, Strategic Systems Projects
Department of the Navy
Washington, D. C. 20376
Attn: LCDR L. Stoessl, SP-272

Naval Plant Representative Office
Lockheed Missiles & Space Co., Inc.
P. O Box 504
Sunnyvale, California 94088
For: Charles Louie III (1)

Avco Corporation
Attn: W. C. Broding
201 Lowell Street
Wilmington, Massachusetts 01887
For: Mr. Joseph R. Wilson, J 300 #2548
Attn: Dr. A. J. Pallone (1)

Commander, Naval Ordnance Laboratory
Attn: Albert Lightbody
White Oak, Silver Springs, Md. 20910
For: Associate Head,
Aero and Hydroballistics
Attn: Dr. R. Kenneth Lobb (1)

Director, USA Ballistic Research Laboratories
Attn: Security Officer
Aberdeen Proving Ground, Md. 21005
For: Dr. C. H. Murphy (1)

AFML/MBC
Wright-Patterson AFB, Ohio 45433
Attn: Mr. Donald L. Schmidt
For: G. L. Denman (1)

Director, Air Force Weapons Laboratory
Kirtland AFB, New Mexico 87117
Attn: SUL, E. Lou Bowman
For Lt. Col. M. W. Hart (1)
Lt. John Gordon

RES-D, General Electric Co.
3198 Chestnut Street
Philadelphia, Pa. 19101
Attn: H. F. Couche, Jr.
For: A. Martellucci,
Valley Forge STC (1)

ARO, Inc.
Attn: Document Control
For: Jack D. Whitfield - VKF
Chief, von Karman Gas Dynamics Facility (1)
Arnold AF Station, Tenn. 37389

1110 J. D. Kennedy
1130 H. E. Viney
1250 J. C. Eckhart
1500 R. L. Peurifoy, Jr.
Attn: 1540 T. B. Lane
1543 H. C. Hardee
1700 O. R. Jones (2)
Attn: 1710 V. E. Blake, Jr.
1720 A. W. Snyder
2334 W. R. Abel
3623 E. R. Frye
4700 D. B. Shuster
4730 R. G. Clem
Attn: 4734 V. L. Dugan
4734 R. D. Klett (8)

DISTRIBUTION (cont):

5000 A. Narath
5100 J. K. Galt
5200 E. H. Beckner
5240 G. Yonas
5600 A. Y. Pope
5628 S. McAlees, Jr.
5700 J. H. Scott
5710 G. E. Brandvold
5720 M. L. Kramm
Attn: 5725 D. J. Rigali
5730 H. M. Stoller
5732 D. A. Northrop
5800 L. M. Berry
5840 D. M. Schuster
Attn: 5842 R. C. Heckman
5846 H. O. Pierson
5846 J. F. Smatana
6011 G. C. Newlin (3)
8100 L. Gutierrez
8110 A. N. Blackwell
8300 B. F. Murphey
9512 R. R. Harnar
8266 E. A. Aas (2)
3141 L. S. Ostrander (5)
3151 W. F. Carstens (3)

For: ERDA/TIC (Unlimited Release)